Depth dependent investigations of thin films and heterostructures with polarized low energy muons

Elvezio Morenzoni

Paul Scherrer Institute
CH-5232 Villigen PSI
Switzerland

- **Generation of polarized low energy muons, beam line and instrument**
- **Selected examples of investigations in near surface region, thin films and heterostructures (superconductivity, magnetism)**

This lecture and a ETH/Univ. ZH course (Physics with muons) on http://people.web.psi.ch/morenzoni/

12th PSI Summer School on
Condensed Matter Research
Zuoz
20.8.2013

Thin films and Heterostructures

- **Fundamental physics**:

• coupling, proximity effects

• coexistence / competition of order parameters

• new electronic states (e.g. surfaces, interfaces)

• dimensional effects

• provide new insight into the intrinsic nature of the constituents

• some materials can be grown only as thin films

- **Technological applications**: Faster, smaller, more efficient devices, new functionalities

Physics characterized by **spatially varying properties on nm (or sub nm) scale**.

We need **probes** that can measure **local magnetic (electronic)** properties of these **regions and access buried layers (LE- muons, β-NMR,….).**

Implantation profiles and ranges

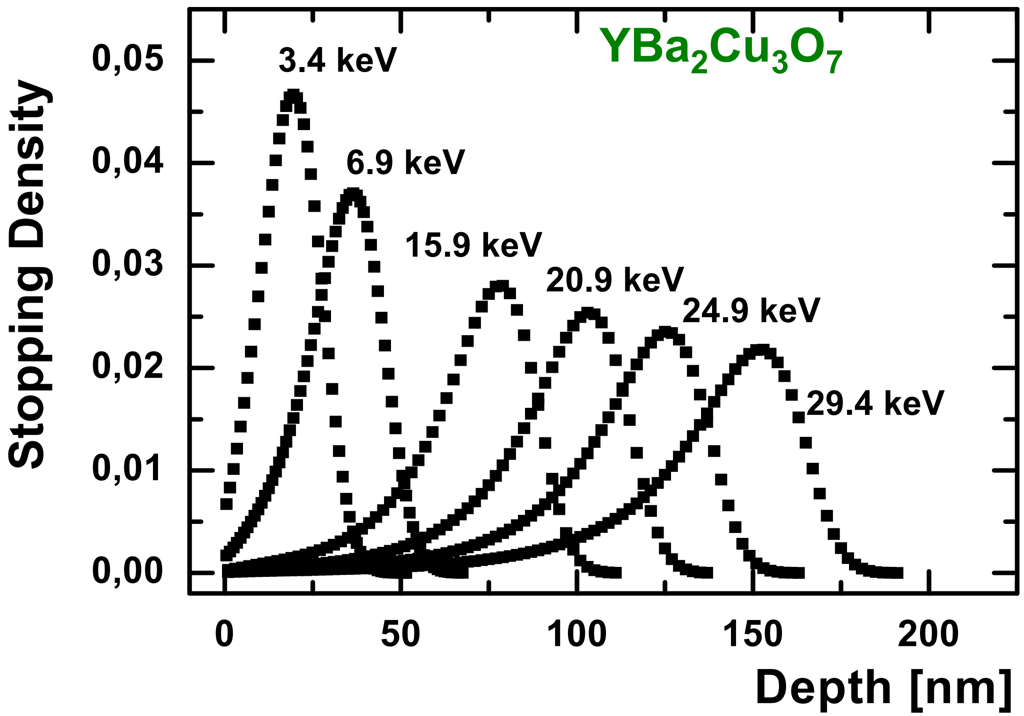

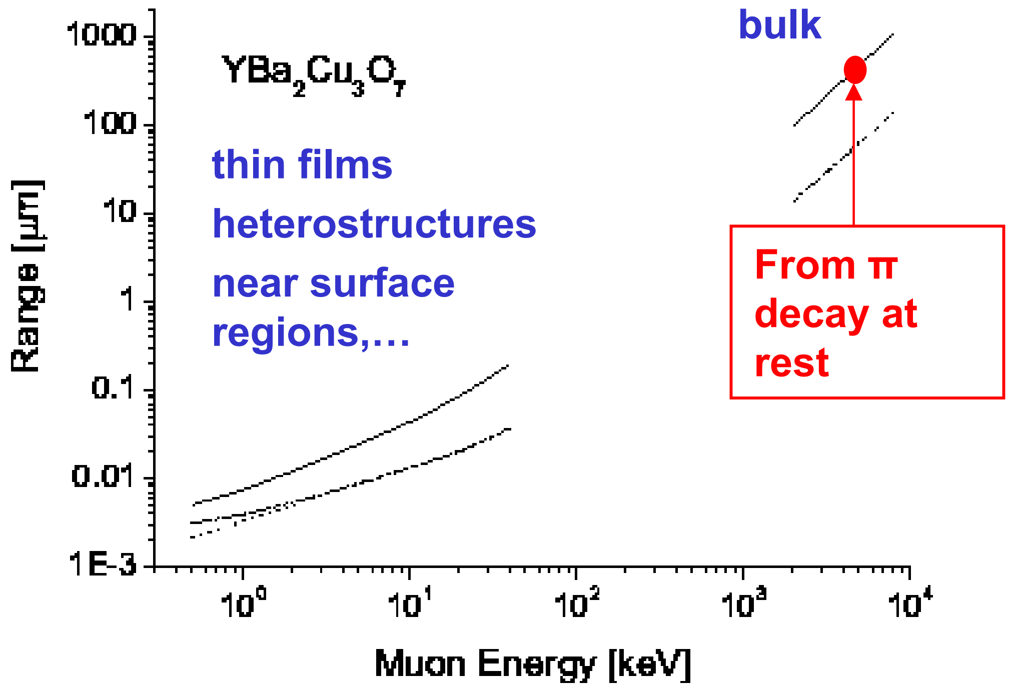

- For thin films studies we need muons with energies in the region of **keV** rather than **MeV**
- Tunable energy (E_μ < 30 keV) allows depth-dependent μSR studies (~ 2 – 300 nm)

Generation of polarized epithermal muons by moderation

„Surface“ Muons

~ 4 MeV

~ 100% polarized

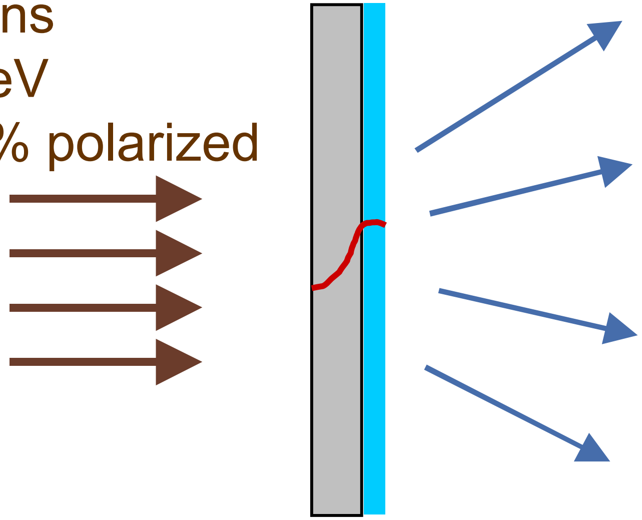

~100 μm Ag

6 K

~ 500 nm

s-Ne, s-Ar

s-N_2

Source of low energy muons (E ~ 15 eV)

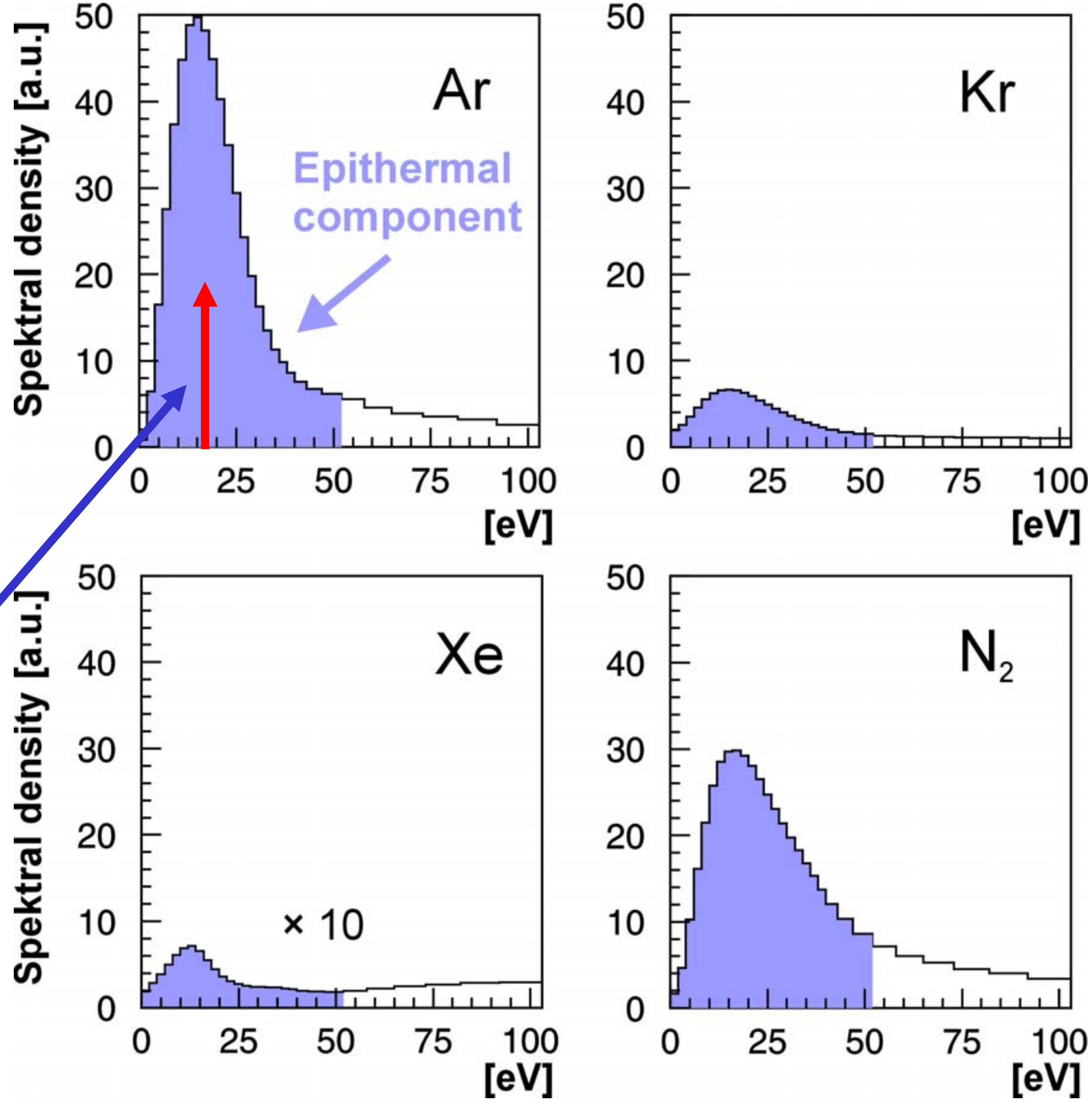

D. Harshmann et al., Phys. Rev. B **36**, 8850 (1987)

E. Morenzoni et al. J. Appl. Phys. **81**, 3340 (1997).

T. Prokscha et al. Appl. Surf. Sci. (2001)

Characteristics of epithermal muons

Polarization 100%

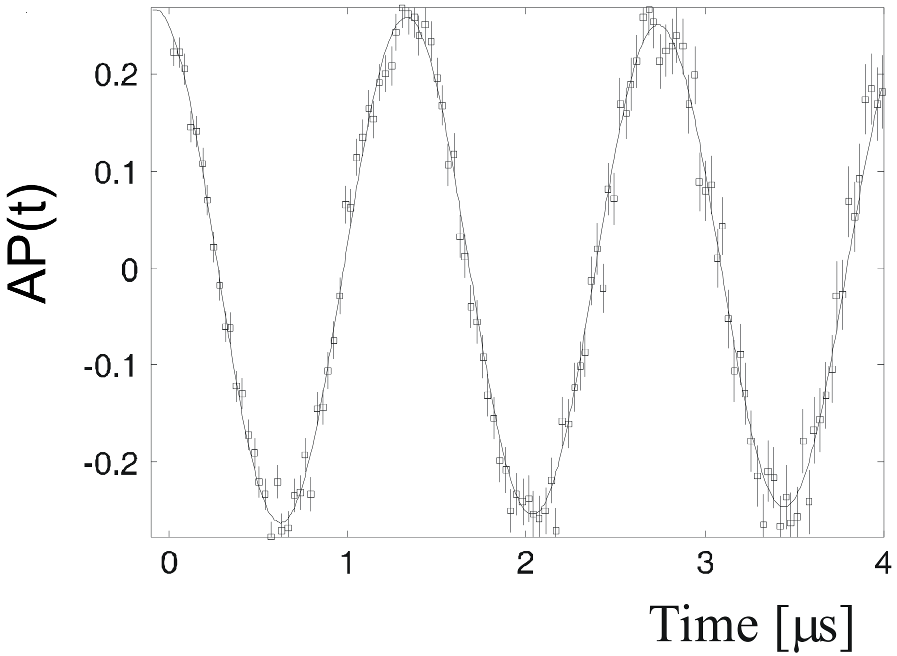

→ Large **escape depth** L (50-250 nm)

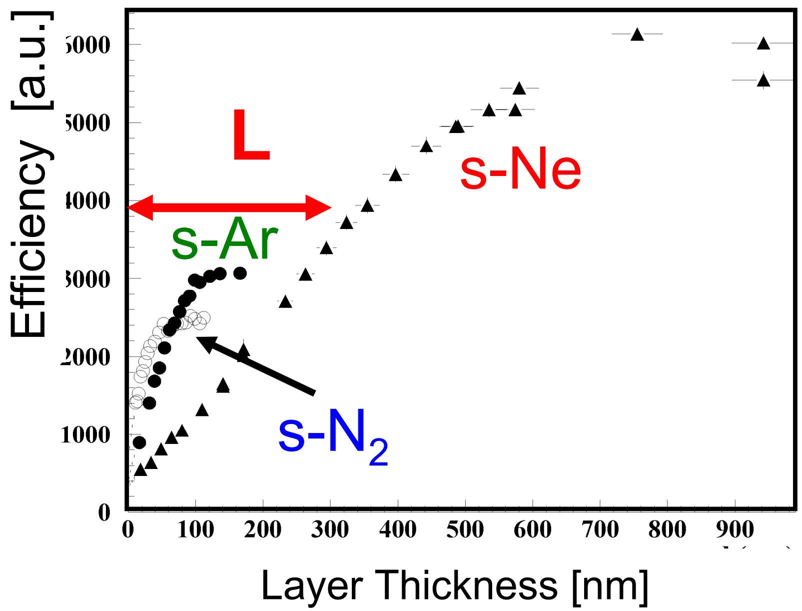

Moderation efficiency:

$$\varepsilon_{\mu^+} \equiv \frac{N_{epith}}{N_{4MeV}} \cong \frac{(1-F_{Mu})L}{\Delta R} \simeq 10^{-4} - 10^{-5}$$

ΔR Stopping width of surface muons $\approx$100 μm

F_{Mu} Muonium formation

Mechanism

Escape of small fraction of muons before thermalization

Suppression of electronic loss processes for $E_\mu \approx E_g$ (wide band gap insulator)

E. Morenzoni, F. Kottmann, D. Maden, B. Matthias, M. Meyberg, Th. Prokscha, Th. Wutzke, U. Zimmermann, Phys.Rev.Lett. **72**, 2793 (1994).

Low energy μ^+ beam and instrument for LE-μSR

- UHV system, 10^{-10} mbar
- some parts LN_2 cooled

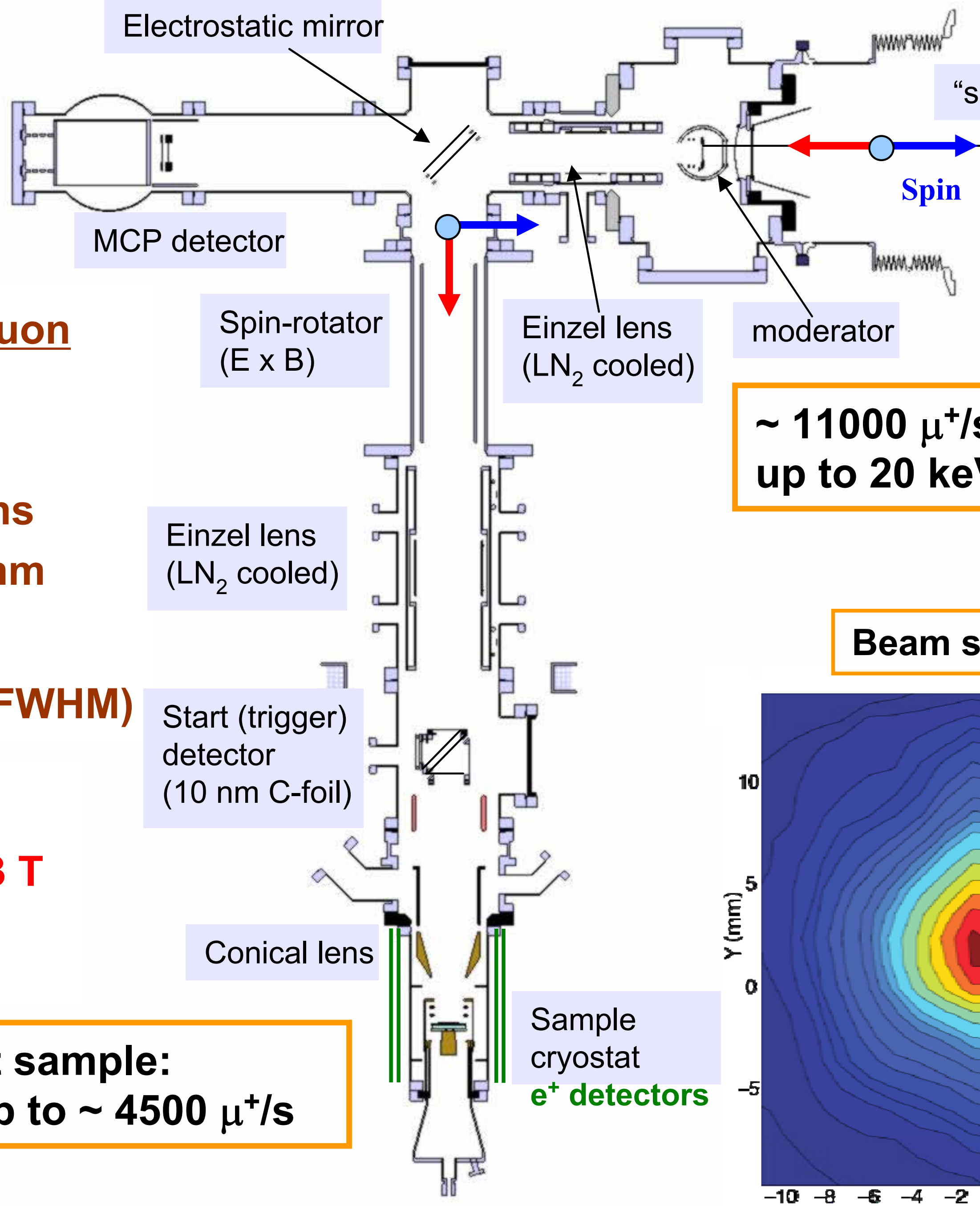

~1.9 • 10^8 μ^+/s

~ 11000 μ^+/s; accelerate up to 20 keV

Polarized Low Energy Muon Beam

Energy:	**0.5-30 keV**
ΔE, Δt:	**400 eV, 5 ns**
Depth:	**~ 2 – 300 nm**
Polarization:	**~ 100 %**
Beam Spot:	**~ 12 mm (FWHM)**

Sample environment:

$B_\perp$ = 0 – 0.3 T, $B_\parallel$ 0 – 0.03 T (to sample surface)

T = 2.5 – 320 K

at sample: up to ~ 4500 μ^+/s

Beam spot at sample

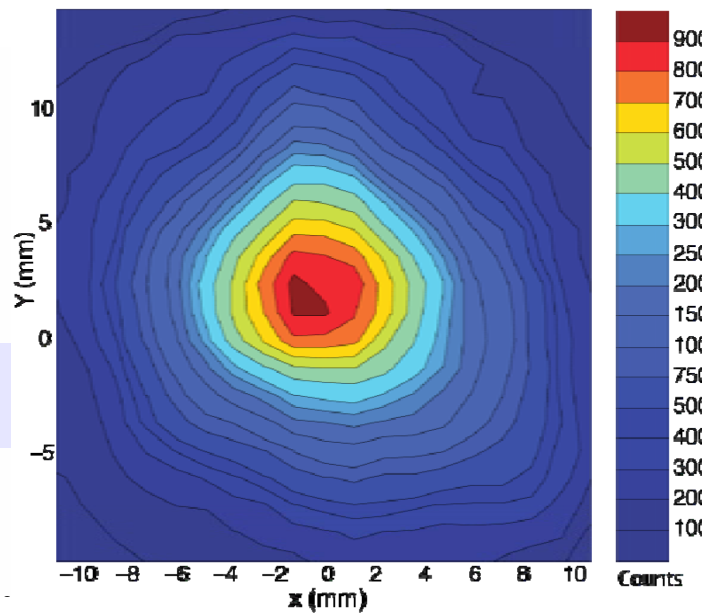

Low energy μ^+ beam and instrument for LE-μSR

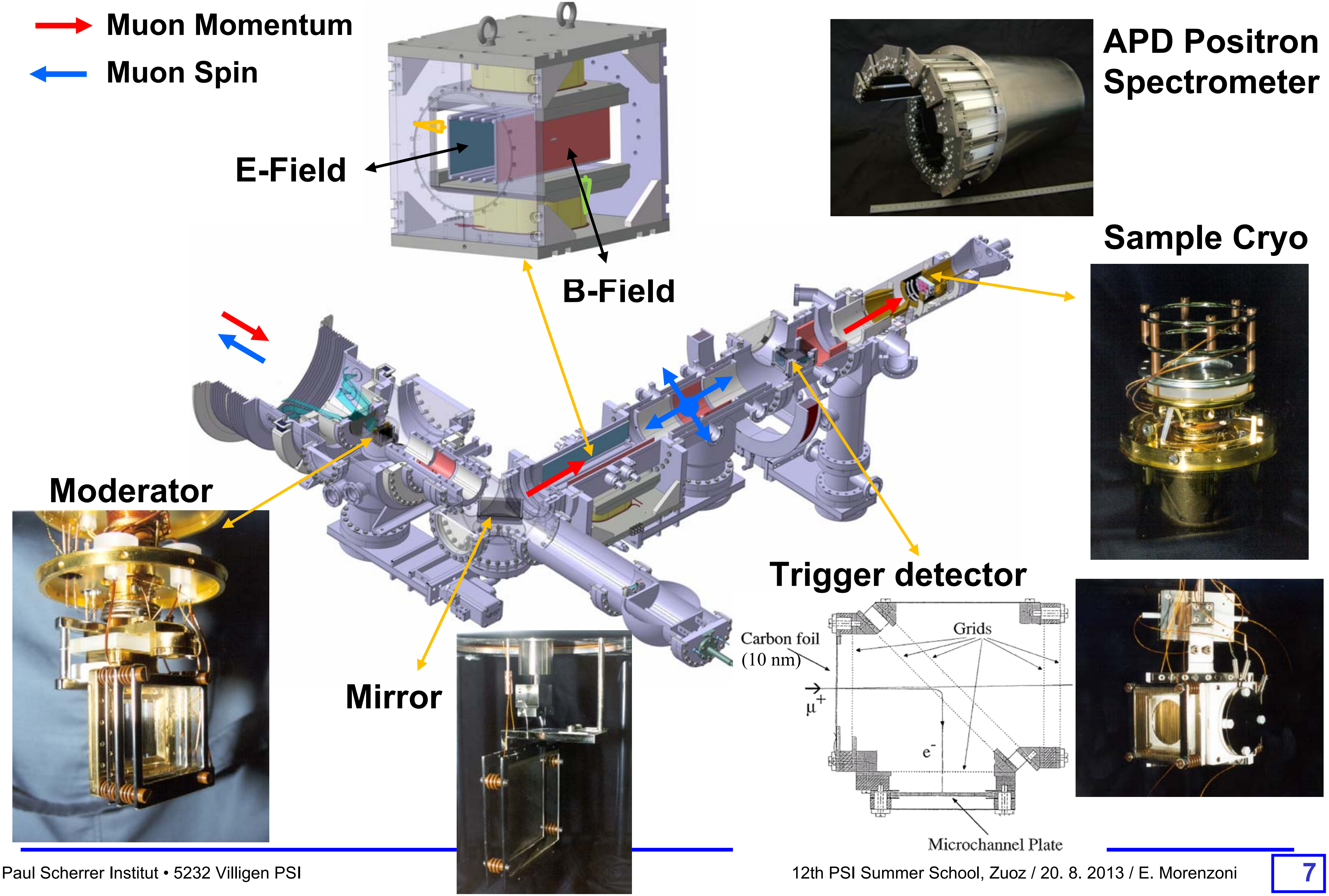

LE-μ^+ Apparatus @ μE4

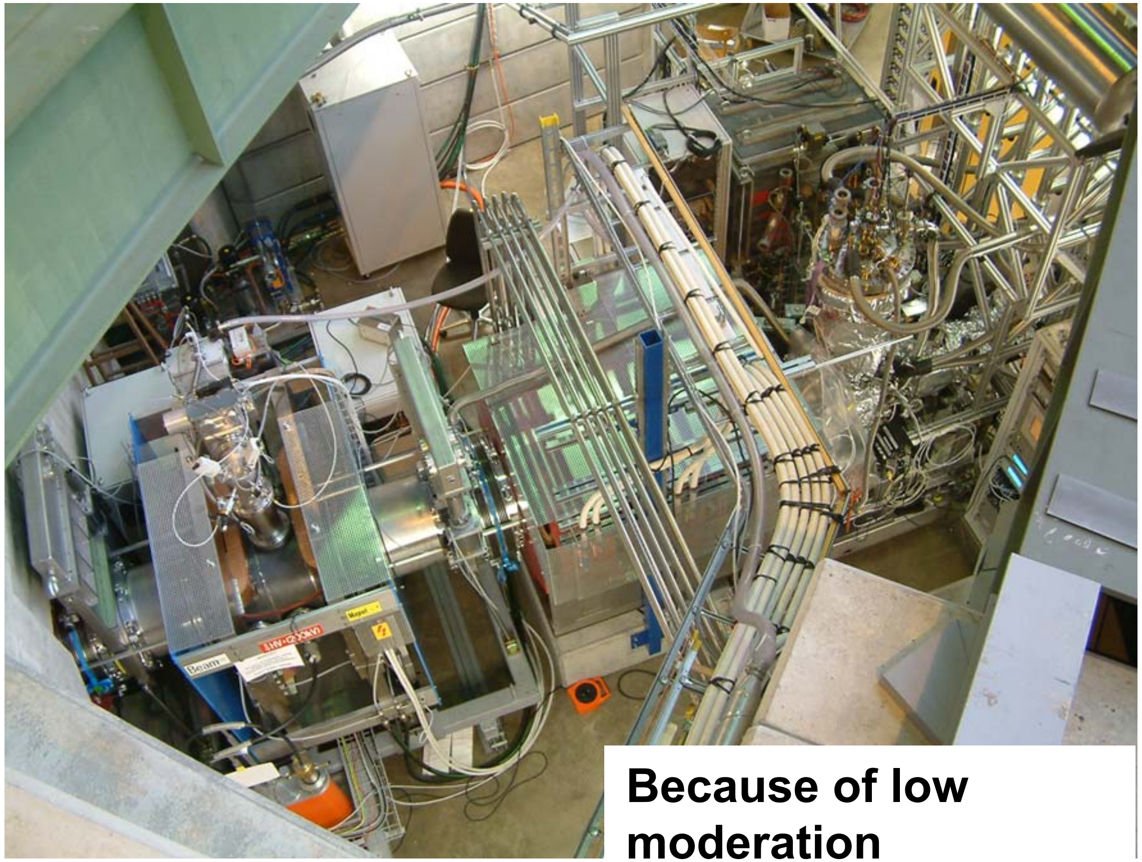

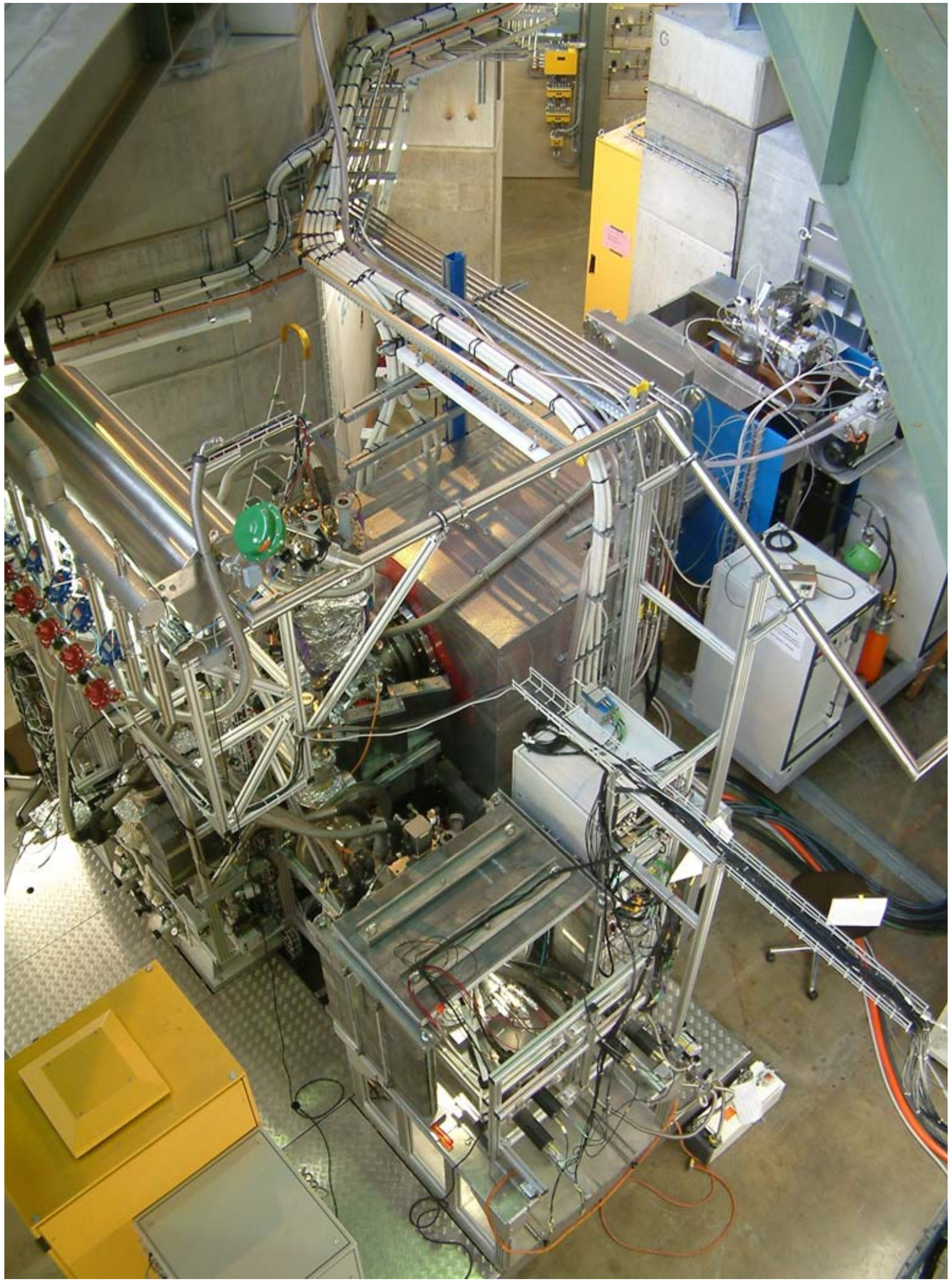

~6 •10^8 μ^+/s total

~1.9 •10^8 μ^+/s on LEM source

Because of low moderation efficiency we need a high flux of "fast" muons: → specially designed beam line μE4 at PSI

Th. Prokscha, E. Morenzoni, K. Deiters, F. Foroughi, D. George, R. Kobler, A. Suter and V. Vrankovic
Physica B 374-375, 460-464 (2006)
and Nucl. Instr. Meth. A 595, 317-331 (2008)

Depth dependent μSR measurements

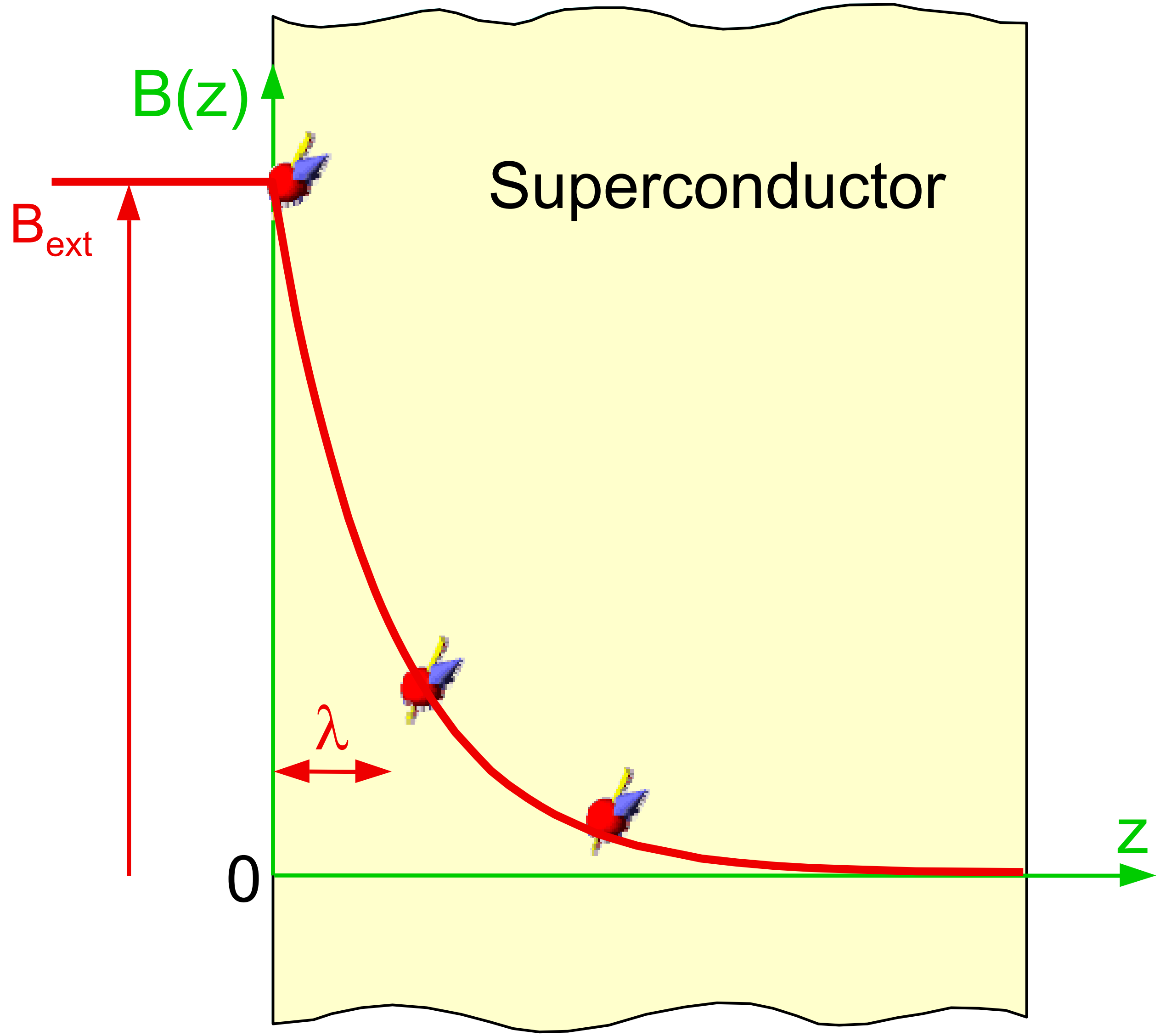

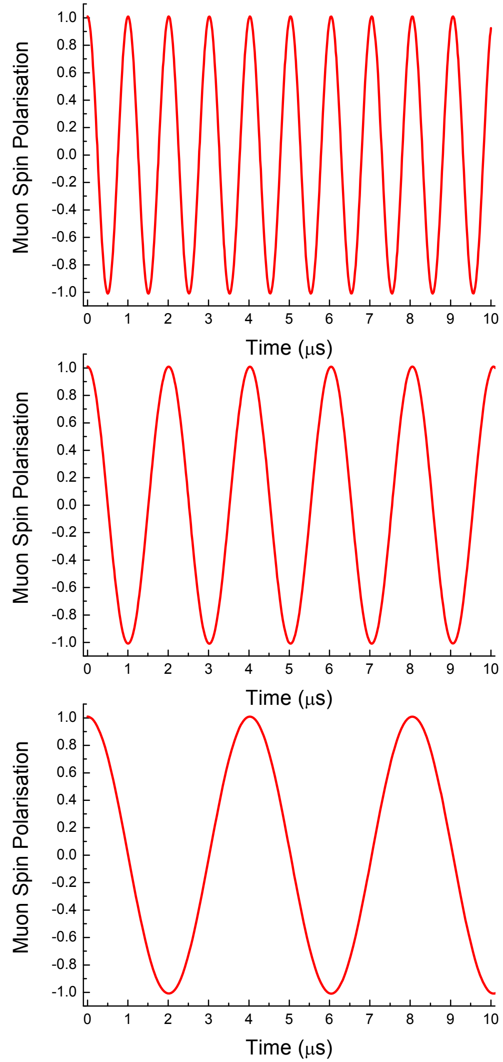

$$\omega_\mu(z) = \gamma_\mu B_{loc}(z)$$

→ Magnetic field profile B(z) over nm scale

<B> vs <z> ⇒ B(z)

Simulating and testing stopping profiles of muons

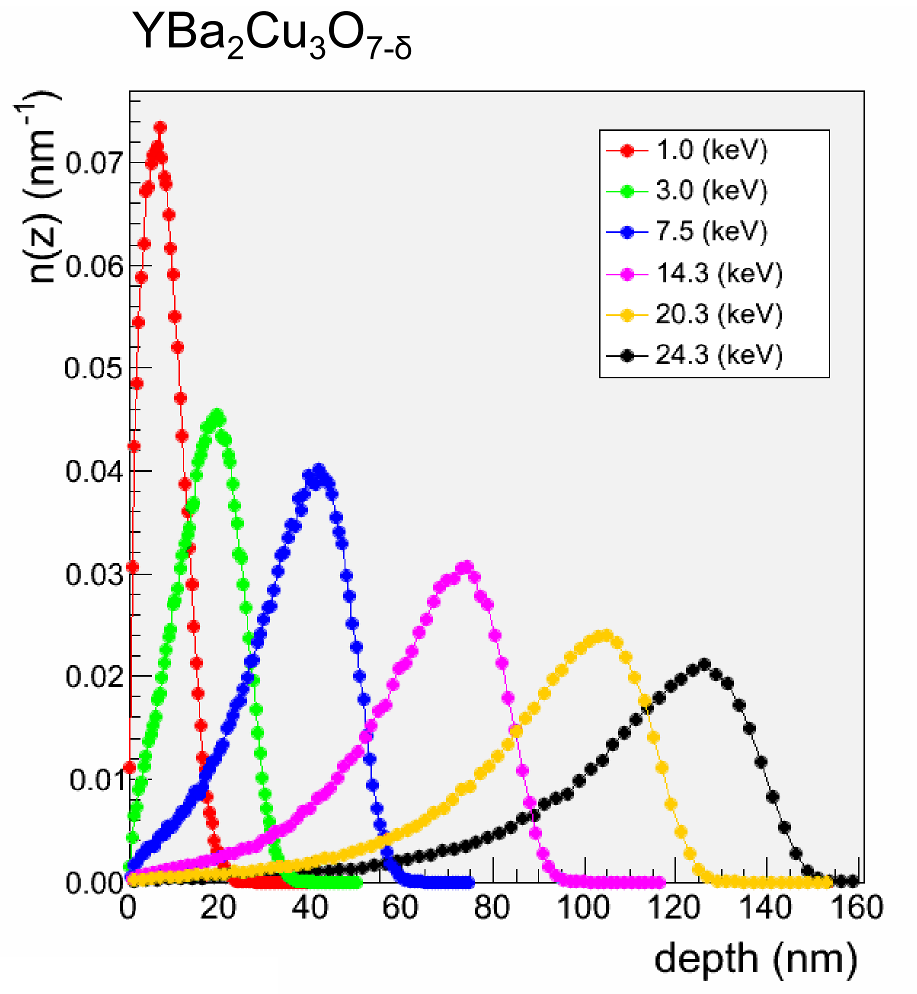

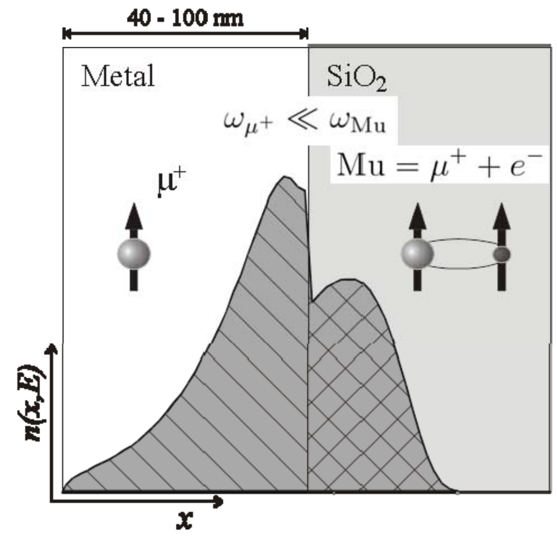

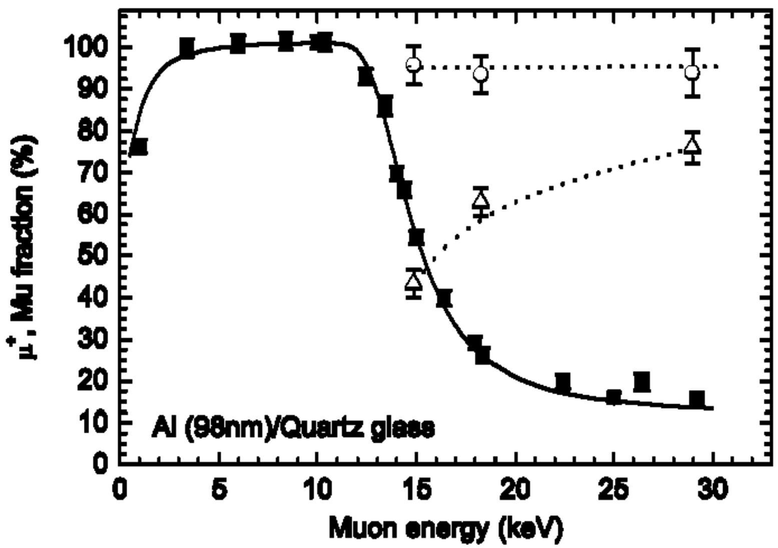

Stopping profiles calculated with the Monte Carlo code Trim.SP W. Eckstein, MPI Garching

Experimentally tested: E. Morenzoni, H. Glückler, T. Prokscha, R. Khasanov, H. Luetkens, M. Birke, E. M. Forgan, Ch. Niedermayer, M. Pleines, NIM B192, 254 (2002).

Examples

Physical object: near surface region, thin film, heterostructure,….

System/Compound

Information and μSR tool used

Examples I

- Near surface region, thin films and heterostructures of unconventional superconductors

- $YBa_2Cu_3O_{6+x}$ and $Ba(Co_xFe_{1-x})_2As_2$ crystals, $La_{2-x}Ce_xCuO_4$ films, $La_{2-x}Sr_xCuO_4$ heterostructures

- magnetic field profiles, magnetic penetration depth, anisotropy, superconducting gap, symmetry, spatial separation of magnetism and superconductivity, proximity effects

- Weak field parallel to surface, $B_{appl} < B_{c1}$, Meissner state, muon spin perpendicular to B

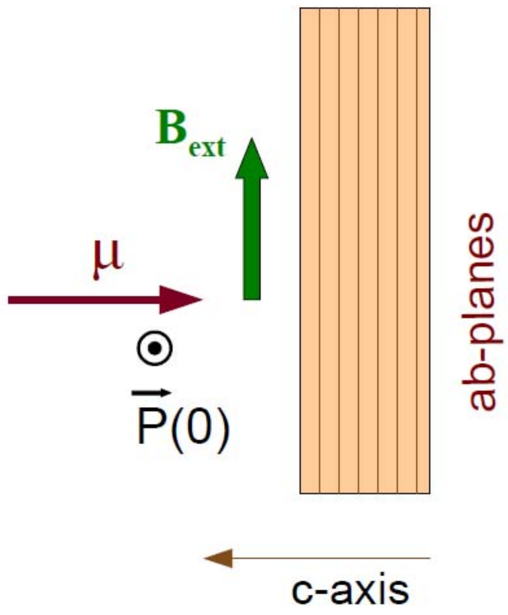

Meissner-Ochsenfeld effect

Magnetic flux is excluded/expelled in the bulk of a superconductor ($B_{appl} < B_{c1}$)

$$\mathbf{B} = \mu_0(\mathbf{H} + \mathbf{M}) = 0$$ perfect diamagnetism

Diamagnetism and zero resistivity described by London equations

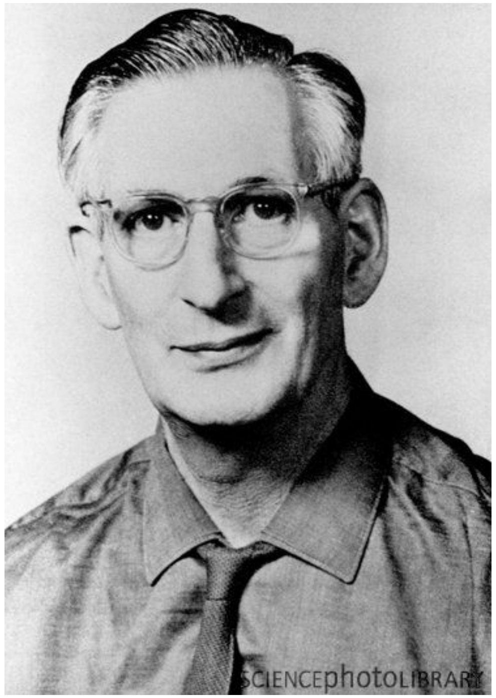

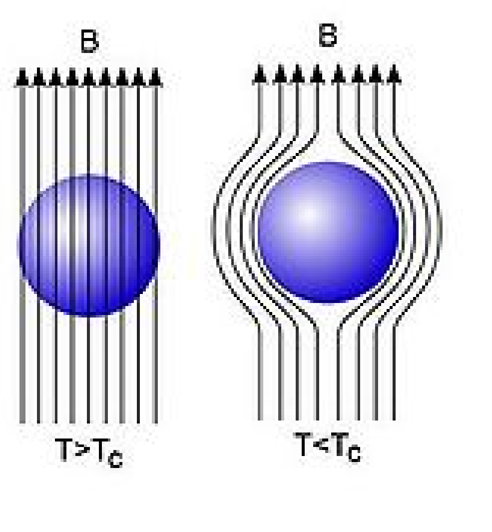

Fritz and Heinz London,
Proc. Roy. Soc. A149, 71 (1935)

London equations

Well describe electrodynamics response of extreme Type II sc, $\lambda >> \xi$ (e.g. cuprates)

1) $$\frac{d\vec{j}}{dt} = \frac{1}{\mu_0 \lambda_L^2}\vec{E}$$

2) $$\mathrm{rot}\,\vec{j} = -\frac{1}{\mu_0 \lambda_L^2}\vec{B} \qquad \left(\vec{j} = -\frac{1}{\mu_0 \lambda_L^2}\vec{A}\right)$$

From 2), $\mathrm{rot}\vec{B} = \mu_0 \vec{j}$ and $\mathrm{rot}(\mathrm{rot}\vec{B}) = \mathrm{grad}\,\mathrm{div}\vec{B} - \Delta\vec{B} \rightarrow \Delta\vec{B} = \frac{1}{\lambda_L^2}\vec{B}$

For $\vec{B}_{appl}$ || surface ($\hat{x}$):

$$B(z) = B_{appl}\, e^{-\frac{z}{\lambda_L}}$$

$$\rightarrow \lambda_L(T) = \sqrt{\frac{m^*}{\mu_0 e^2 n_s(T)}}$$ (in "clean limit" $\ell >> \xi_0$)

λ_L magnetic penetration depth (London)

m^*, n_S effective mass and density of superconducting carriers

Magnetic field (and shielding current) penetrate the superconductor to a small extent: magnetic penetration depth λ_L (or λ)

Magnetic penetration depth

Dependence of magnetic penetration depth λ on T, B_{appl}, orientation, composition.. gives information about microscopic properties of superconductor (order parameter, gap symmetry, anisotropy,..)

Two complementary methods:

Determination from **Vortex state** (A. Amato talk) based on:

-theory describing vortex state (Ginzburg-Landau, London, …) relating measured field distribution p(B) (or its moments) with λ

-regular vortex lattice (symmetry)

-take into account effects of field, non-local, non-linear, influence of disorder

-very efficient and quick

Determination from **Meissner state**:

-gives absolute value without assumptions on the sc state

-needs good films or flat crystals

-measurements more time consuming

λ_a , λ_b anisotropy in $YBa_2Cu_3O_{6+x}$

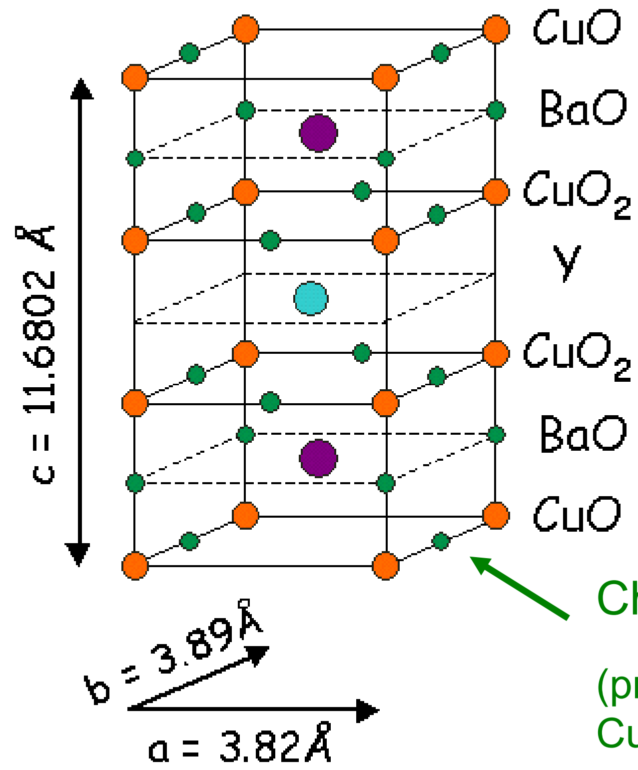

Chain Oxygen x

(provide carriers to CuO_2 planes)

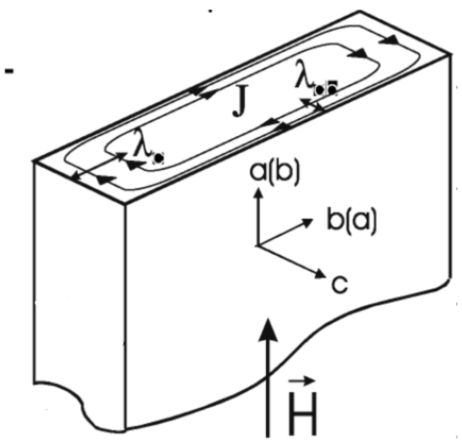

Field decay determined by shielding current flowing in $\hat{a}$ or $\hat{b}$

$\vec{H}_{ext} \parallel \hat{a}\text{-axis} \rightarrow \lambda_b$

$\vec{H}_{ext} \parallel \hat{b}\text{-axis} \rightarrow \lambda_a$

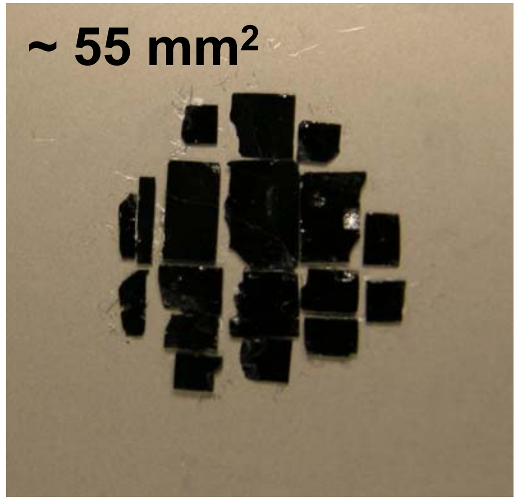

Ultraclean $YBa_2Cu_3O_{6+x}$ crystals

(T_c= 94.1 K, $\Delta T_c \lesssim$ 0.1K @OP)

Detwinning factor > 95%

x=0.92	Optimally doped
x=0.998	Ortho I
x=0.52	Ortho II

samples produced by
R. Liang, W. Hardy, D. Bonn,
Univ. of British Columbia

μSR Spectra: $A(t)=A_0P(t)$

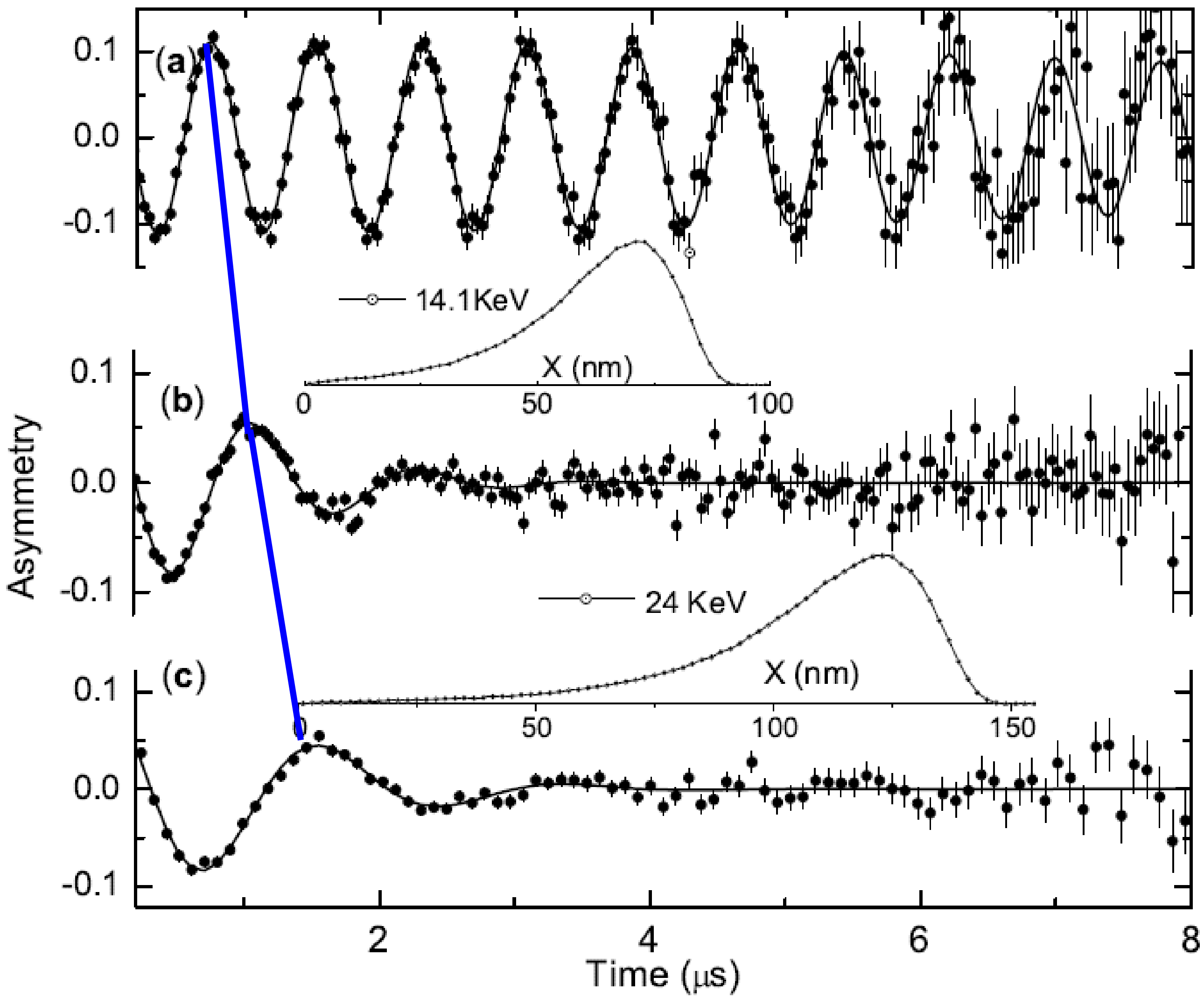

$\vec{B}_{appl} = 9.47\text{mT} \quad || \ \hat{a}\text{-axis}$

$T = 110\ K$

$T = 8\ K$

$$\mathcal{A}(t) = A \exp\left[-\sigma^2 t^2/2\right] \int \rho(z) \cos\left[\gamma_\mu B(z)t + \phi\right]\ dz \qquad B(z) = \begin{cases} B_0 \exp\left[-(z-d)/\lambda_{a,b}\right] & , z \geqslant d \\ B_0 & , z < d\,, \end{cases}$$

Field profiles

$YBa_2Cu_3O_{6.92}$

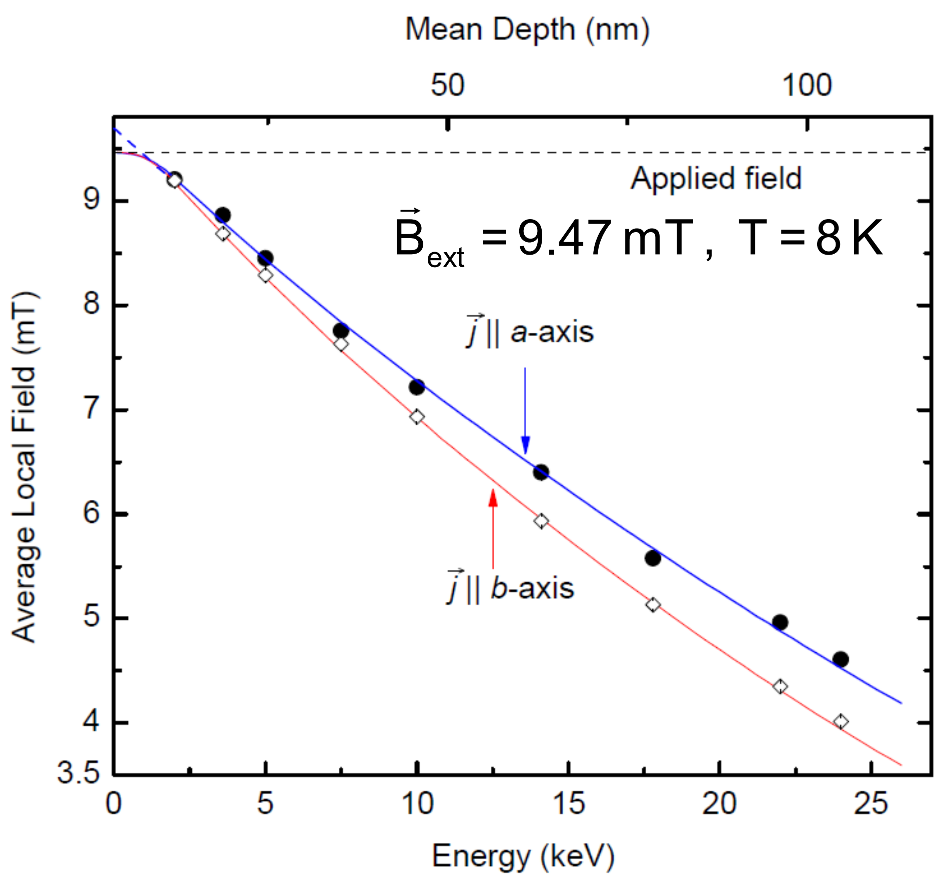

Ortho I: $YBa_2Cu_3O_{6.998}$

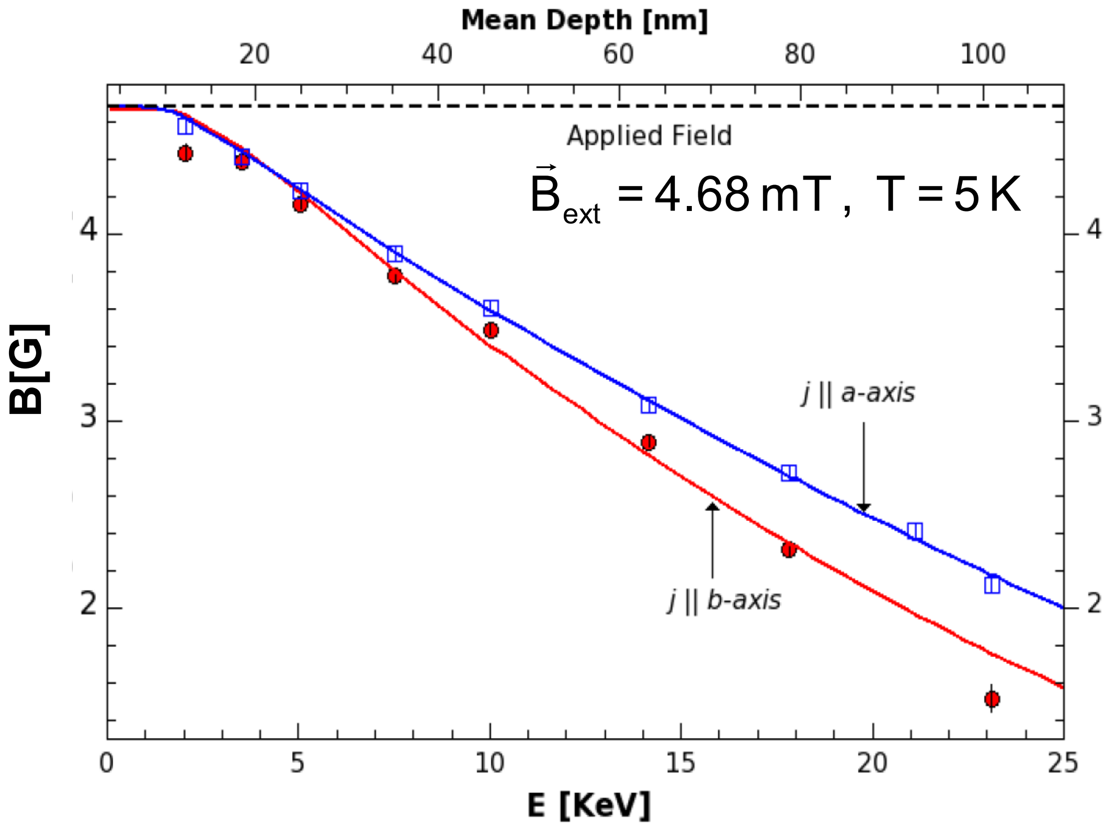

R. Kiefl et al. , Phys. Rev. **B81**, 180502(R) (2010)

An iron-based sc (122): $Ba(Co_xFe_{1-x})_2As_2$

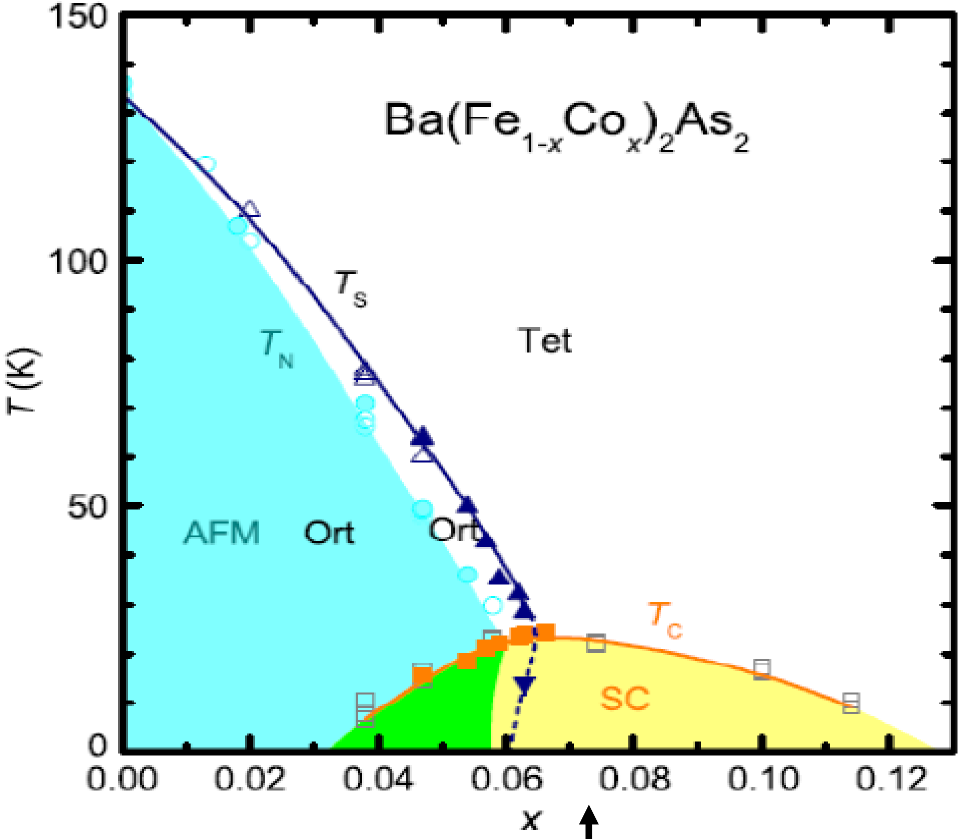

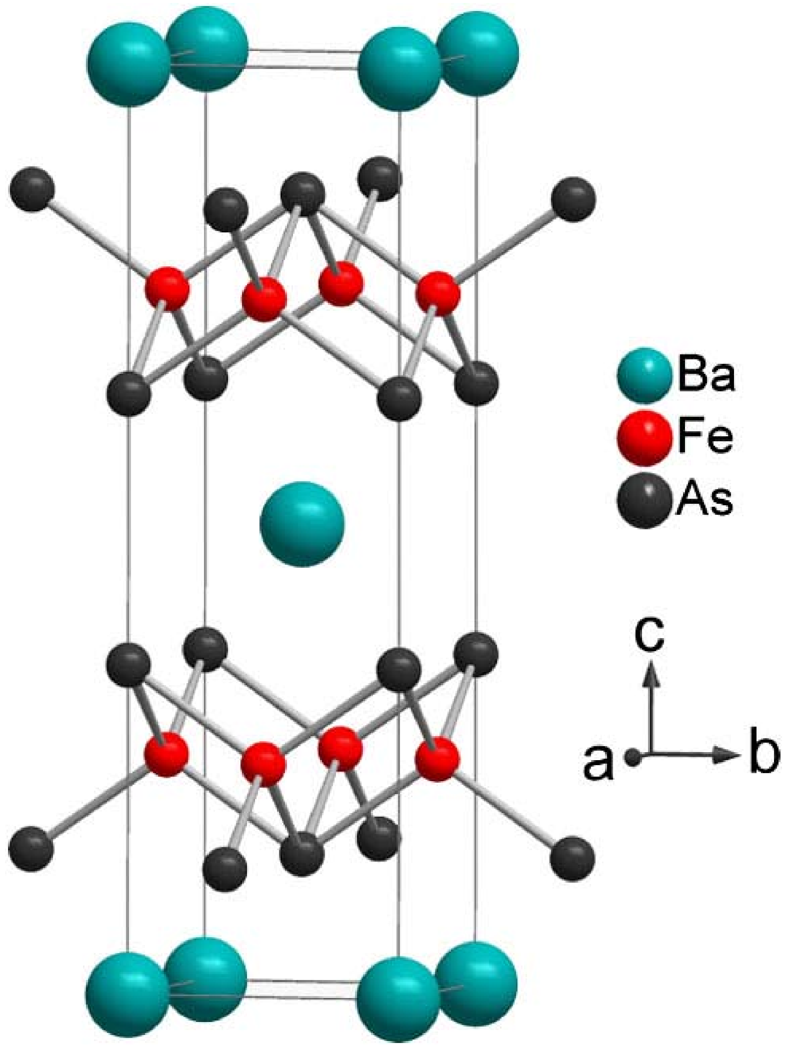

$Ba(Co_{0.074}Fe_{0.926})_2As_2$

T_c=21.7 K, ΔT_c=0.8 K

S. Nandi et al., PRL 104, 057006 (2009)

Fermi surface and superconducting gap

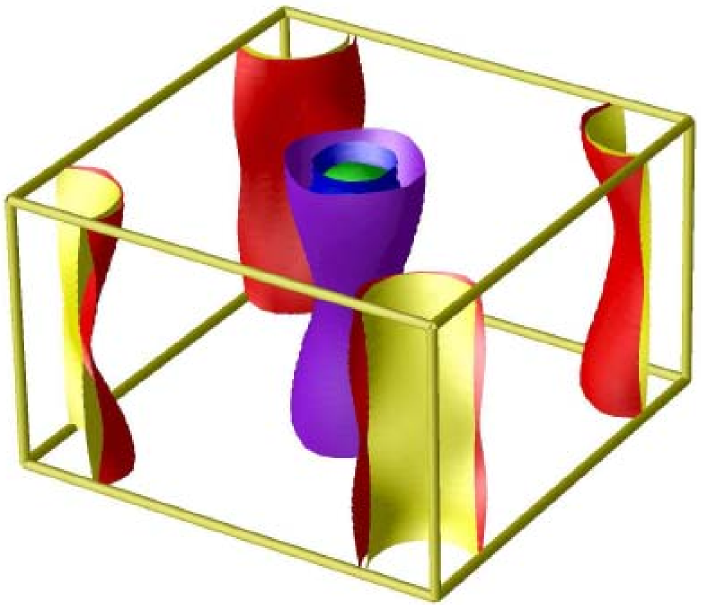

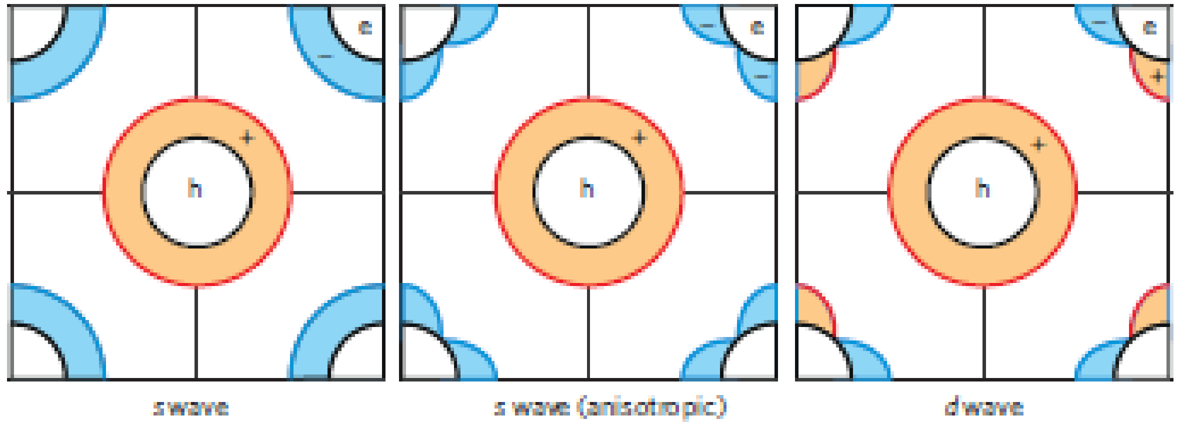

s+/-

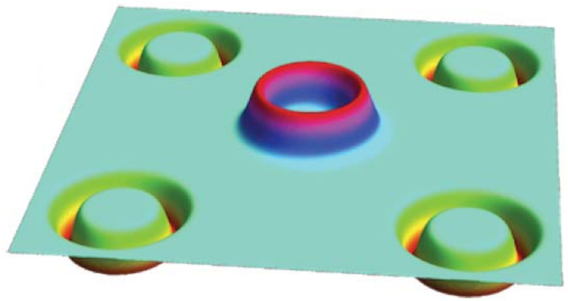

From J. Paglione, R.L. Green, Nat. Phys. 2010

Superfluid density ρ(T)

Superfluid density:

$$\frac{1}{\lambda(T)^2} \propto \frac{n_S(T)}{m^*} \equiv \rho_S(T)$$

Normalized superfluid density:

$$\rho(T)=\frac{\lambda^2(0)}{\lambda^2(T)}=(1+\frac{\Delta\lambda(T)}{\lambda(0)})^{-2} \qquad \Delta\lambda(T)=\lambda(T)-\lambda(0)$$

Ex.: 2D cylindrical Fermi surface:

$$\rho_{bb}^{aa}(T)=1-\frac{1}{2\pi T}\int_0^{2\pi}\begin{pmatrix}\cos^2(\varphi)\\ \sin^2(\varphi)\end{pmatrix}\int_0^{\infty}\cosh^{-2}\left(\frac{\sqrt{\varepsilon^2+\Delta^2(T,\varphi)}}{2T}\right)d\varepsilon d\varphi$$

s – wave gap:

$\Delta(T,\varphi)=\Delta(T)$

d – wave gap:

$\Delta(T,\varphi)=\Delta(T)\cos(2\varphi)$

$$\tan\varphi=\frac{k_y}{k_x}$$

$\sqrt{\varepsilon^2+\Delta^2(T,\varphi)}$: quasiparticle energy

$$\varepsilon=\frac{\hbar^2k^2}{2m^*}$$

$\Delta(T,\varphi)$: superconducting gap

Magnetic penetration depth

$Ba(Co_{0.074}Fe_{0.926})_2As_2$

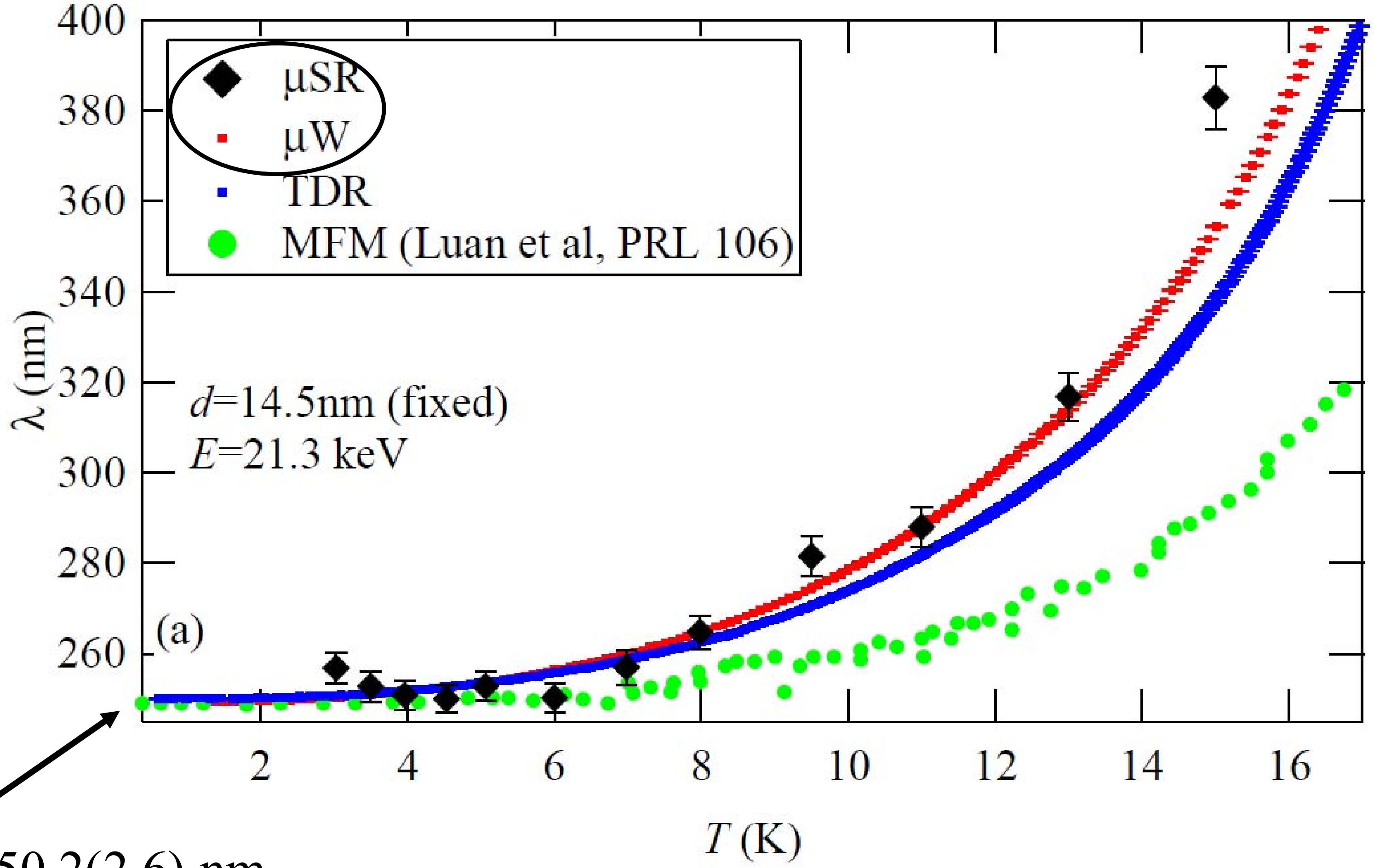

$\lambda(0) = 250.2(2.6)$ nm

+ 3% Stopping profile uncertainty

Combination of LE-μSR and microwave absorption (μW) measurement → **λ(0)** , **Δλ(T)**

O. Ofer et al., Physical Review **B 85**, 060506(R) (2012)

Superfluid density ρ(T)

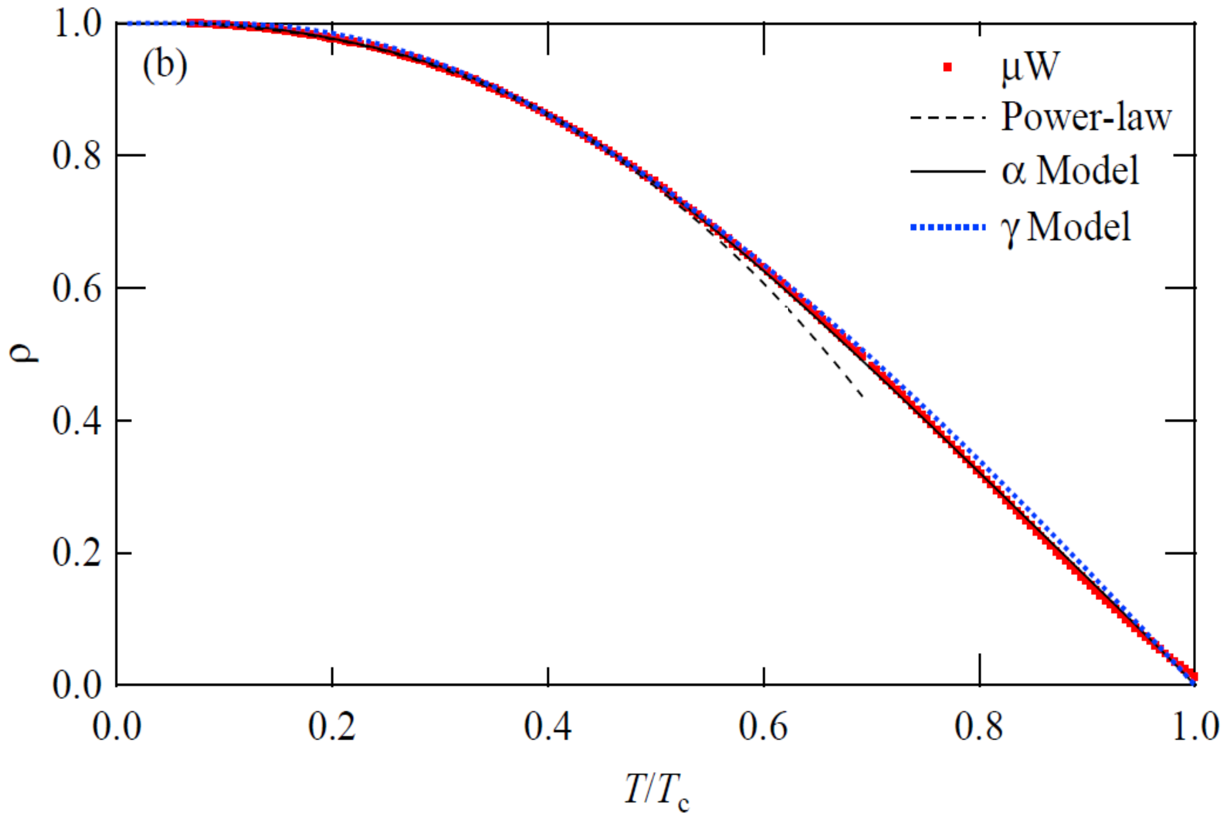

Data well fitted with two s-wave gaps (s+/-)

$$\frac{2\Delta_L(0)}{k_B T_c} = 3.46(10) \qquad \text{BCS ratio} = \frac{\pi}{e^{\gamma}} \cong 3.53$$

$$\frac{2\Delta_S(0)}{k_B T_c} = 1.20(7) \qquad \text{with } 9.7(1)\ \%\ \text{weight}$$

Competition and separation of phases in $La_{2-x}Ce_xCuO_4$

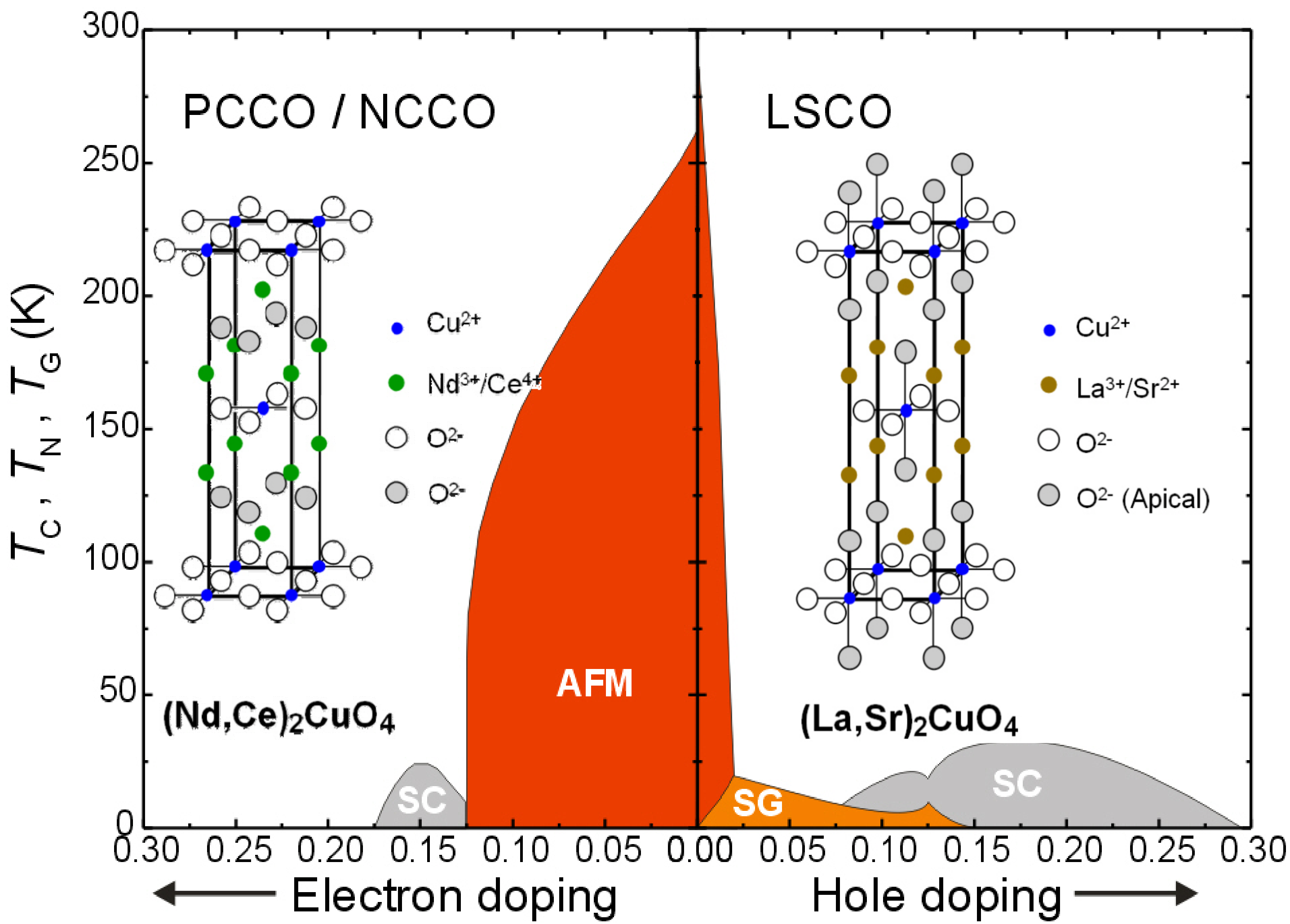

$Nd^{3+} \rightarrow Ce^{4+}$ $La^{3+} \rightarrow Sr^{2+}$

$La^{3+} \rightarrow Ce^{4+}$ (thin film)

$La_{2-x}Ce_xCuO_4$ thin film

x = 0.02 - 0.04, Antiferromagnetic

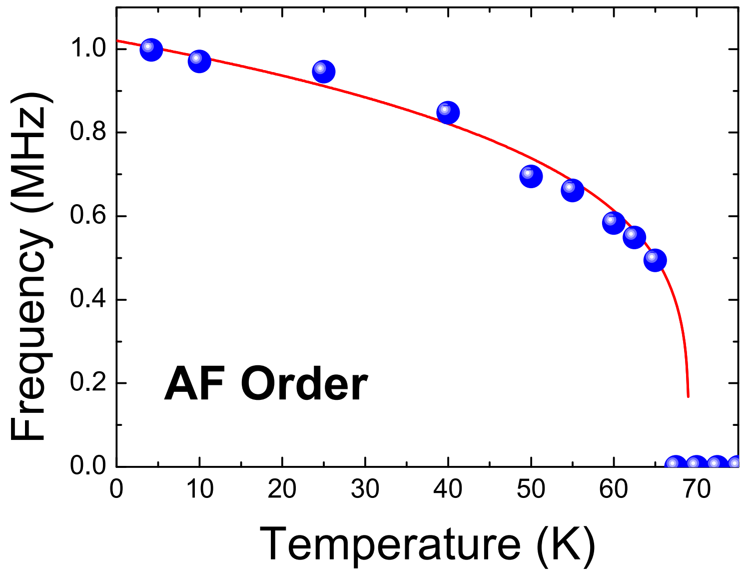

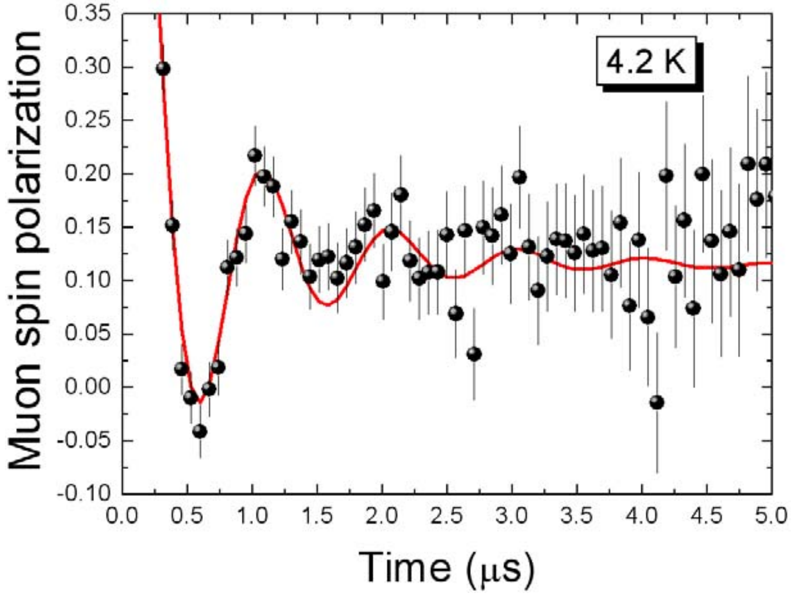

x=0.135 (overdoped) **superconducting no magnetism**

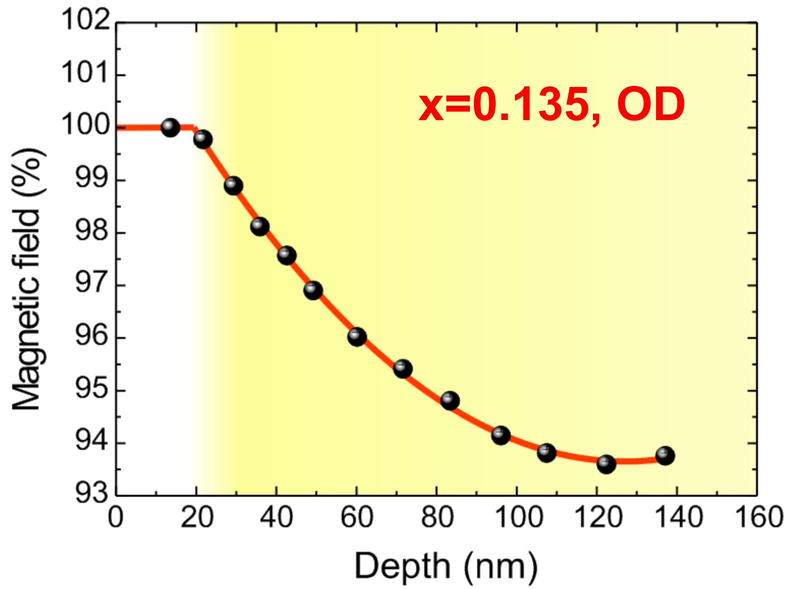

H. Luetkens, Y. Krockenberger et al.,

Phase diagram of $La_{2-x}Ce_xCuO_4$

TF **x=0.0825 (optimally doped)**

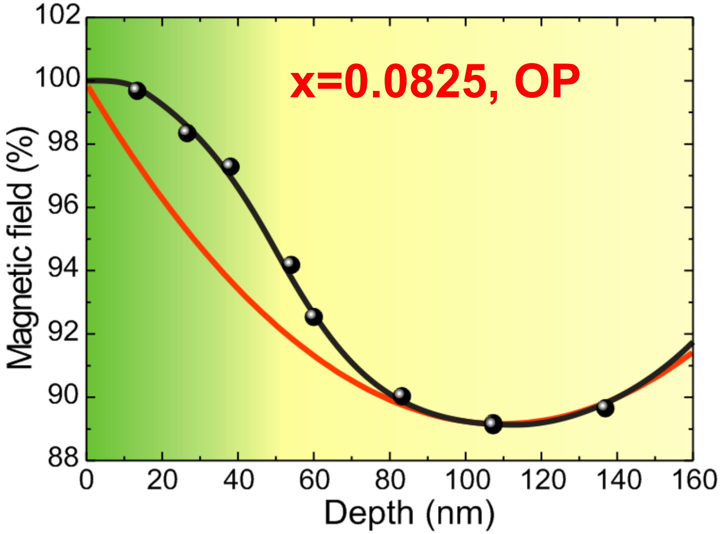

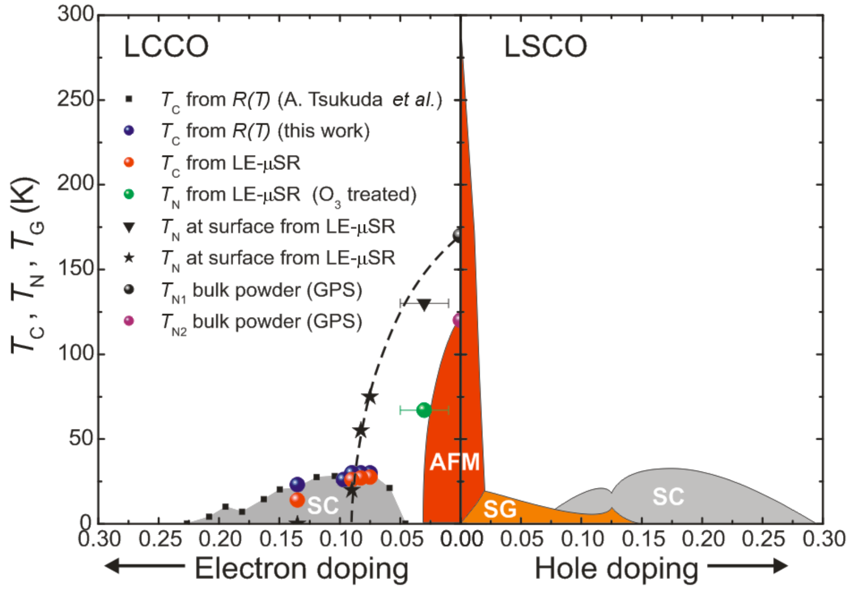

ZF

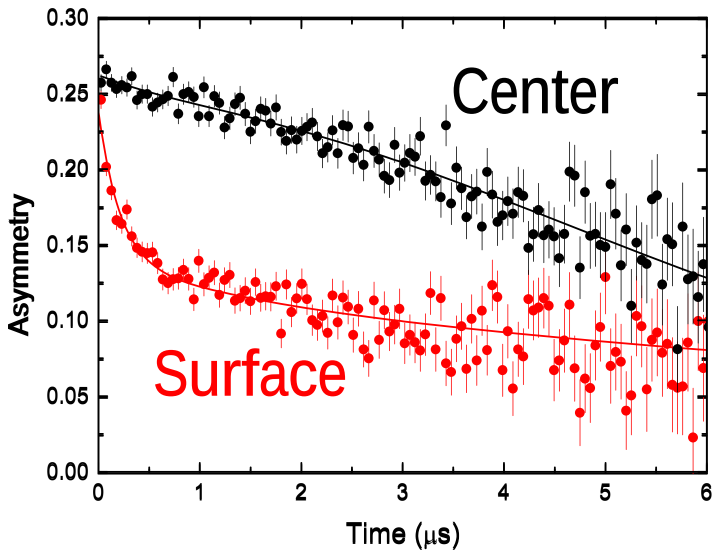

x=0.075 (underdoped)

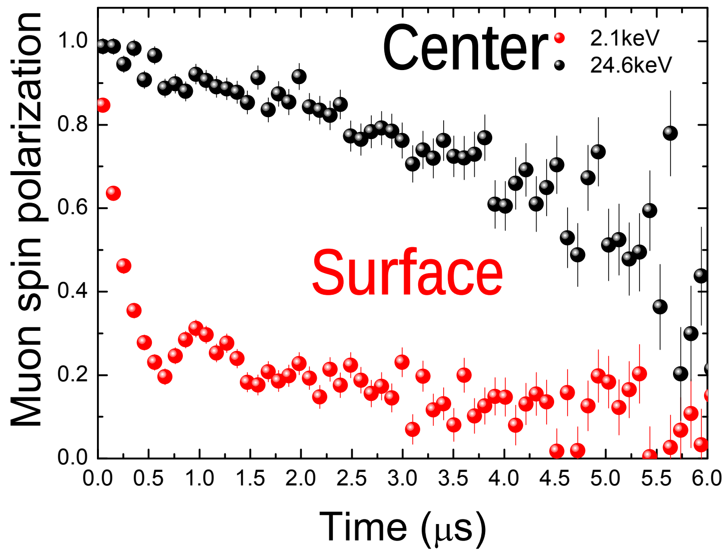

Magnetic surface, superconducting center. Coexistence of both in the same sample. Competing orders.

Several tests indicate that the formation of the magnetic layer is intrinsic.

$La_{1.84}Sr_{0.16}CuO_4$ / $La_{1.94}Sr_{0.06}CuO_4$ / $La_{1.84}Sr_{0.16}CuO_4$

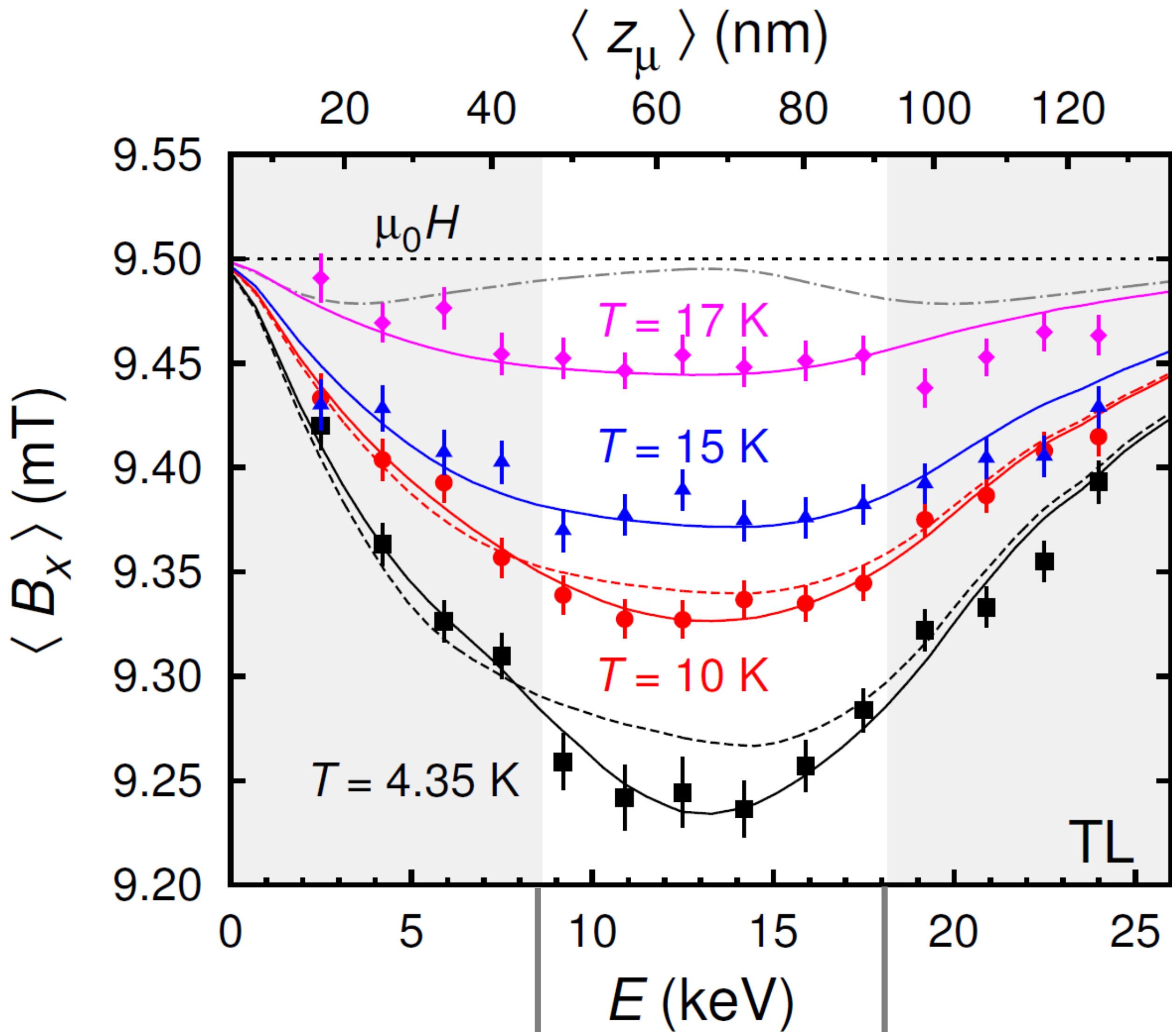

$La_{1.84}Sr_{0.16}CuO_4$
46nm **$T_c \cong$ 32 K**

$La_{1.94}Sr_{0.06}CuO_4$
46nm **$T_c' <$ 5K**

$La_{1.84}Sr_{0.16}CuO_4$
46nm **$T_c \cong$ 32 K**

Giant proximity effect:

Field exclusion in a "non-superconducting" thick layer embedded in two superconductors

$$d \gg \xi_c \simeq 0.3 \text{ nm},$$

$$d \gg \xi_N = \sqrt{\frac{\hbar v_c \ell}{2\pi k_B (T - T_c')}} \leq 3 \text{ nm}$$

(for T $\geq$ 10K)

E.Morenzoni., B. Wojek, A. Suter, T. Prokscha, G. Logvenov, I. Božovic, *Nat. Commun.* 2:272 (2011).

Example II

- Thin films (MBE) of diluted magnetic semiconductors, (GaMn)As

- Intrinsic spatial inhomogeneity (phase separation?) or homogeneous magneticground state?, Strength of ferromagnetic interaction

- Weak transverse field, zero field

DMS: diluted magnetic semiconductors

Semiconductor, where small concentration of magnetically active element doped at a cation site.

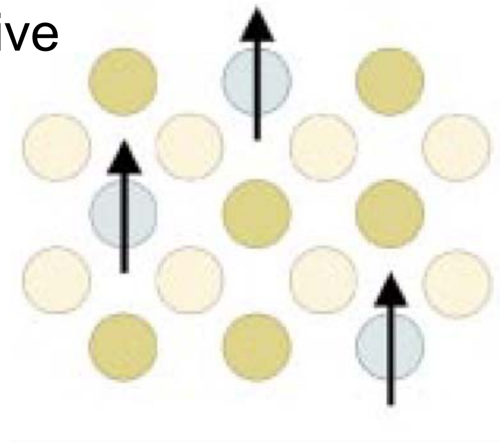

Semiconducting (information processing)

and ferromagnetic properties (storage)

→ spintronics (see Talk T. Jungwirth)

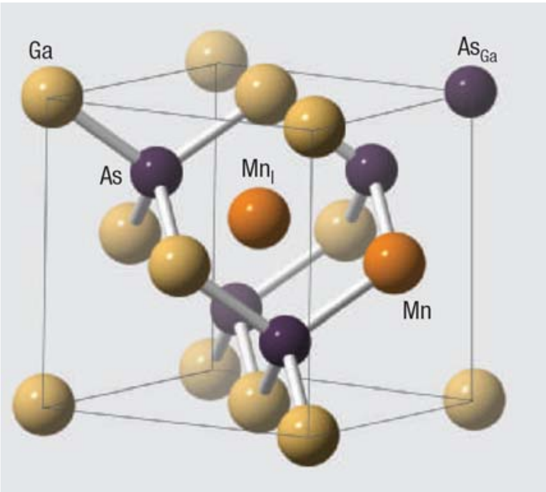

$Ga_{1-x}Mn_xAs$

Mn^{2+} @ Ga^{3+} site:
magnetic moment + hole

→FM semiconductor

*(H. Ohno, Science **281**, 951 (1998))*

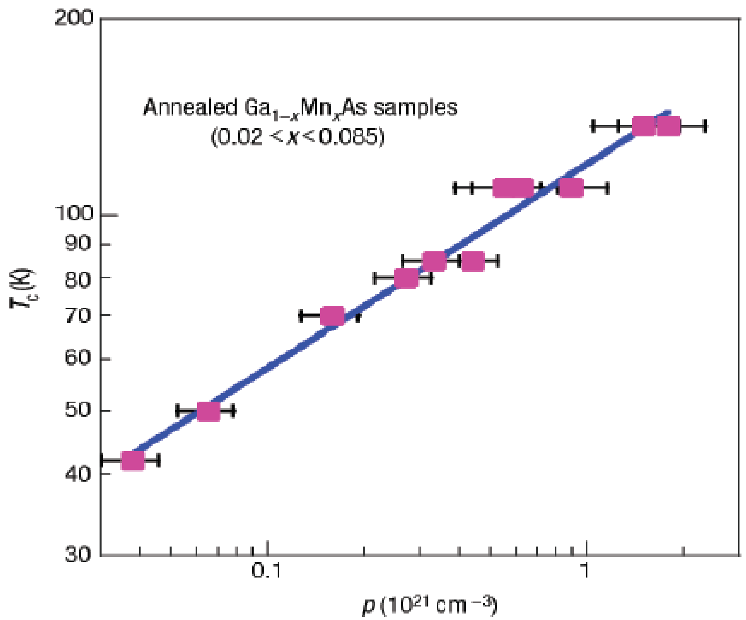

Can be grown only as thin films, low temp. MBE

Electric field control of magnetism

Electric field control of magnetism, *H. Ohno et al.* *Nature* **408**, 944 (2000)

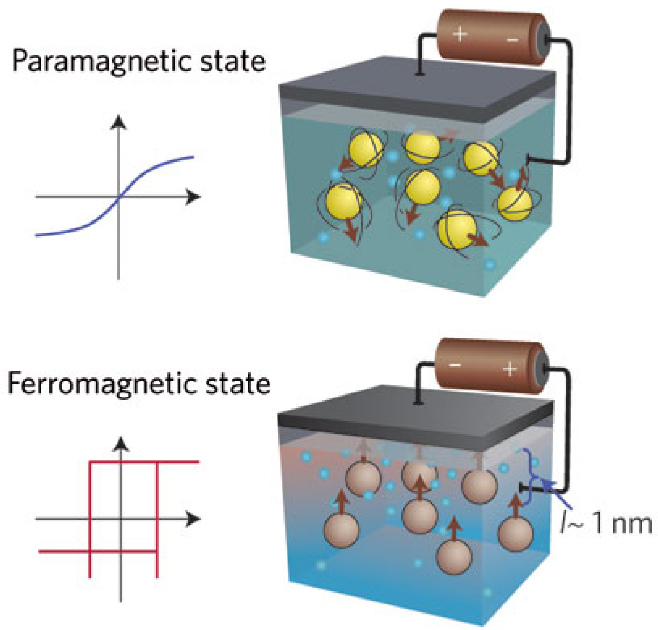

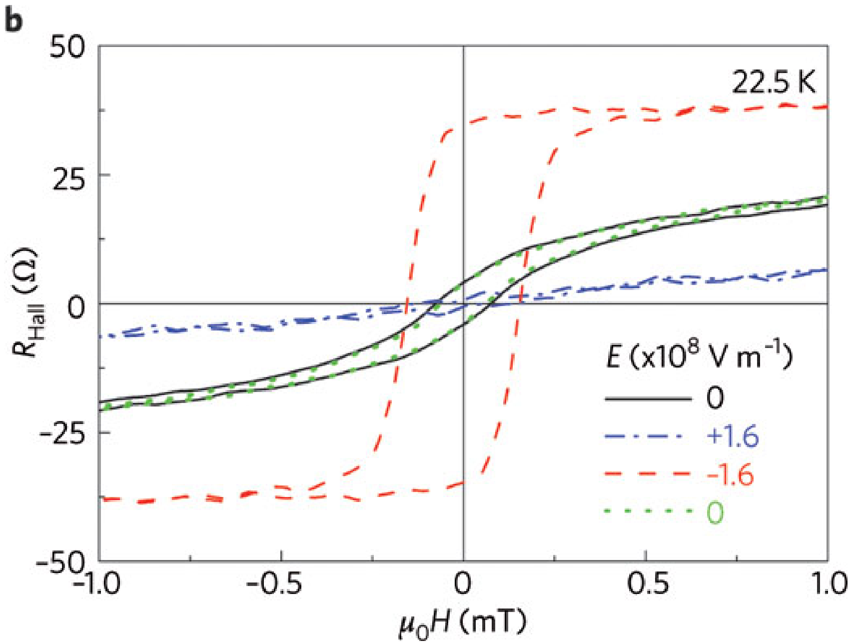

Magnetization vector manipulation by electric fields, *D. Chiba et al.* *Nature* **455**, 515-518 (2008)

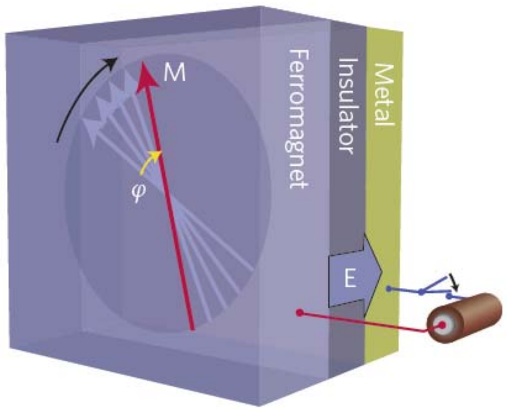

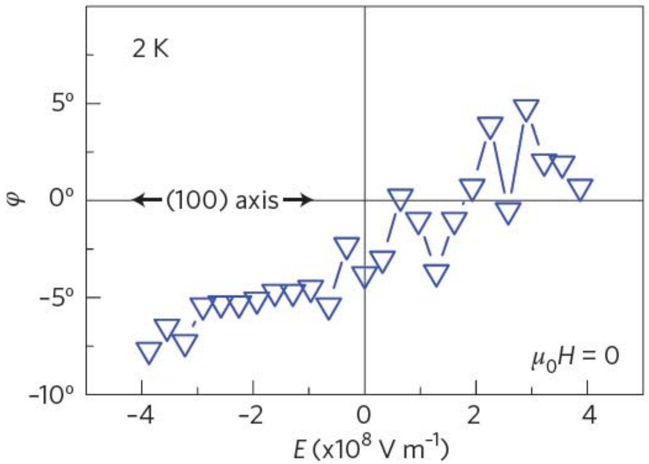

Spatially homogeneous ferromagnetism?

a

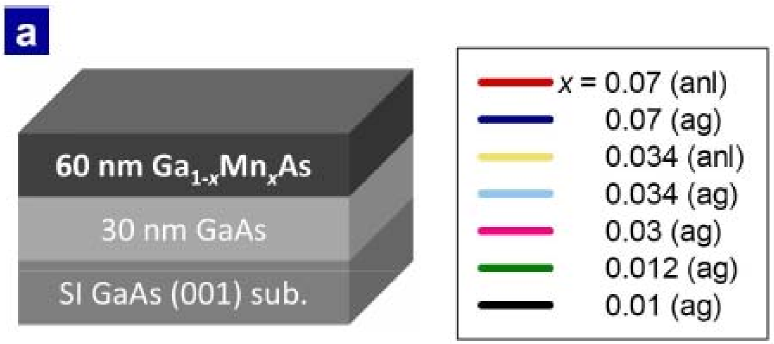

b

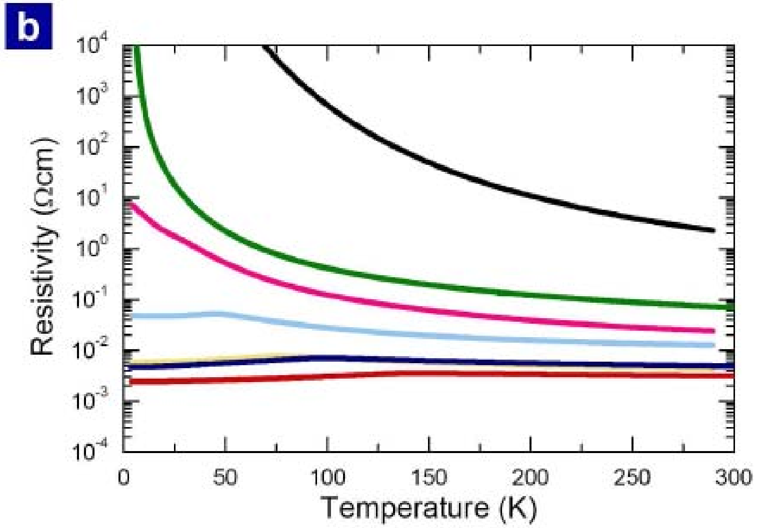

c

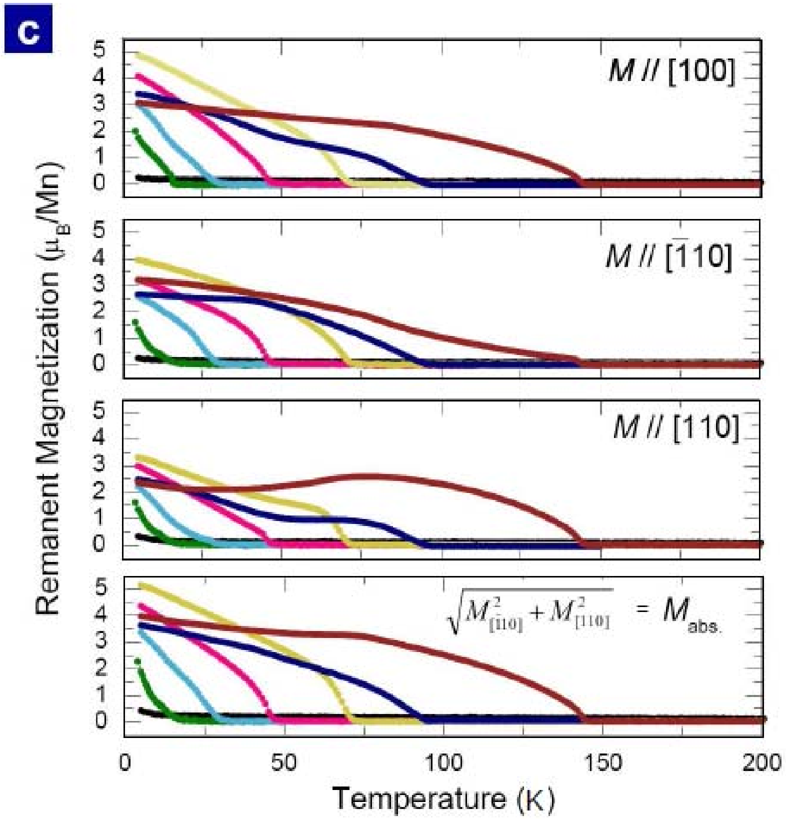

Sample	x = 0.010 as-grown	0.012 as-grown	0.030 as-grown	0.034 as-grown	0.034 annealed	0.070 as-grown	0.070 annealed
T_c from M	< 5 K	16 K	29 K	46 K	73 K	96 K	146 K
T_c from ρ	-	-	-	45 K	76 K	97 K	145 K

Properties highly sensitive to preparation condition and heat treatment

→ Nature of FM state: unavoidable and instrinsic strong spatial inhomogeneities or homogeneous ground state?

→ Evolution from paramagnetic insulator to ferromagnetic metal

Determining the magnetic volume fraction

In case of two phases (e.g. a magnetic and a non-magnetic) the μSR signal will be:

$$A(t) = f\ A_S G_{Mag}(t) + (1-f) A_S G_{nonMag}(t) + A_{Bg}$$

The magnetic fraction f can be easily determined in a wTF measurements

$$B_{appl} << B_{Mag}(M)$$

$T>T_C$ $f=0$ (PM Phase, $G_{nonMag}(t) \approx 1$):

$$A(t) = A_S \cos(\gamma_\mu Bt + \varphi) + A_{Bg} \cos(\gamma_\mu B_{appl} t + \varphi) \qquad B = B_{appl} + \langle B_{PM} \rangle$$

$$\uparrow = 0$$

$T< T_C$:

$$A_{osc}(t) = (1-f)\ A_S \cos(\gamma_\mu Bt + \varphi) + A_{Bg} \cos(\gamma_\mu B_{appl} t + \varphi)$$

When the applied field is larger than the internal static fields sensed by the muons, the amplitude of the asymmetry component oscillating in the applied field represents para- / non-magnetic volume (+ Bg)

Determining the magnetic volume fraction

Weak Transverse Field 10mT

T>T_C

T<T_C

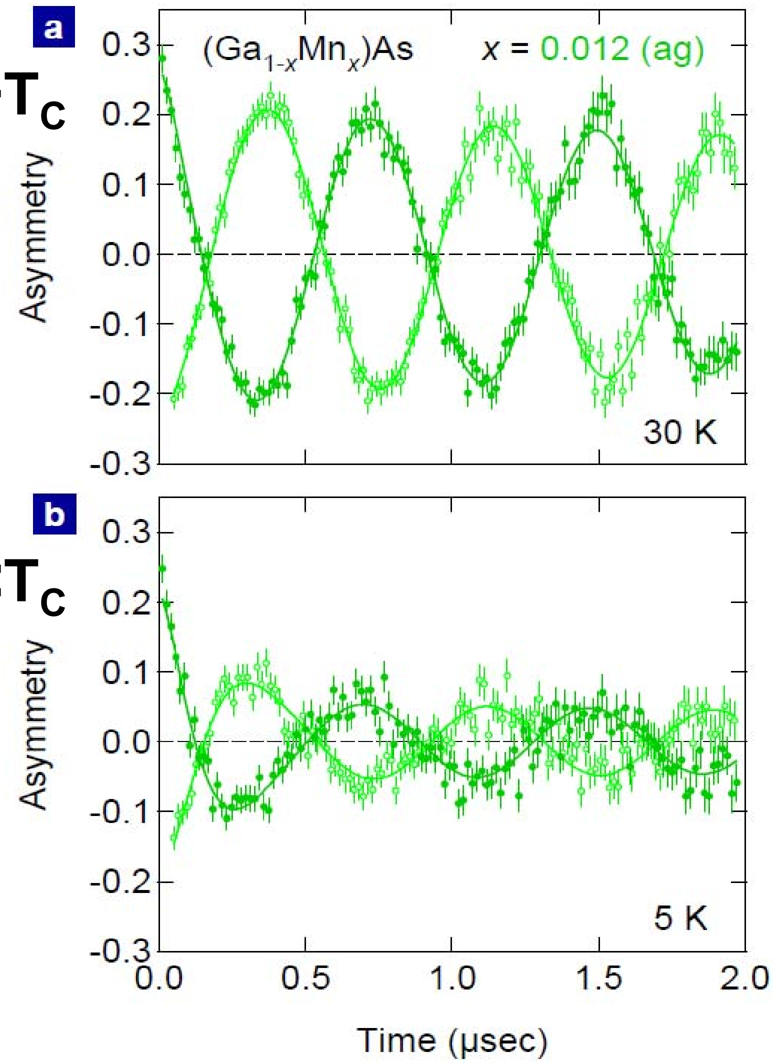

Magnetic volume fraction

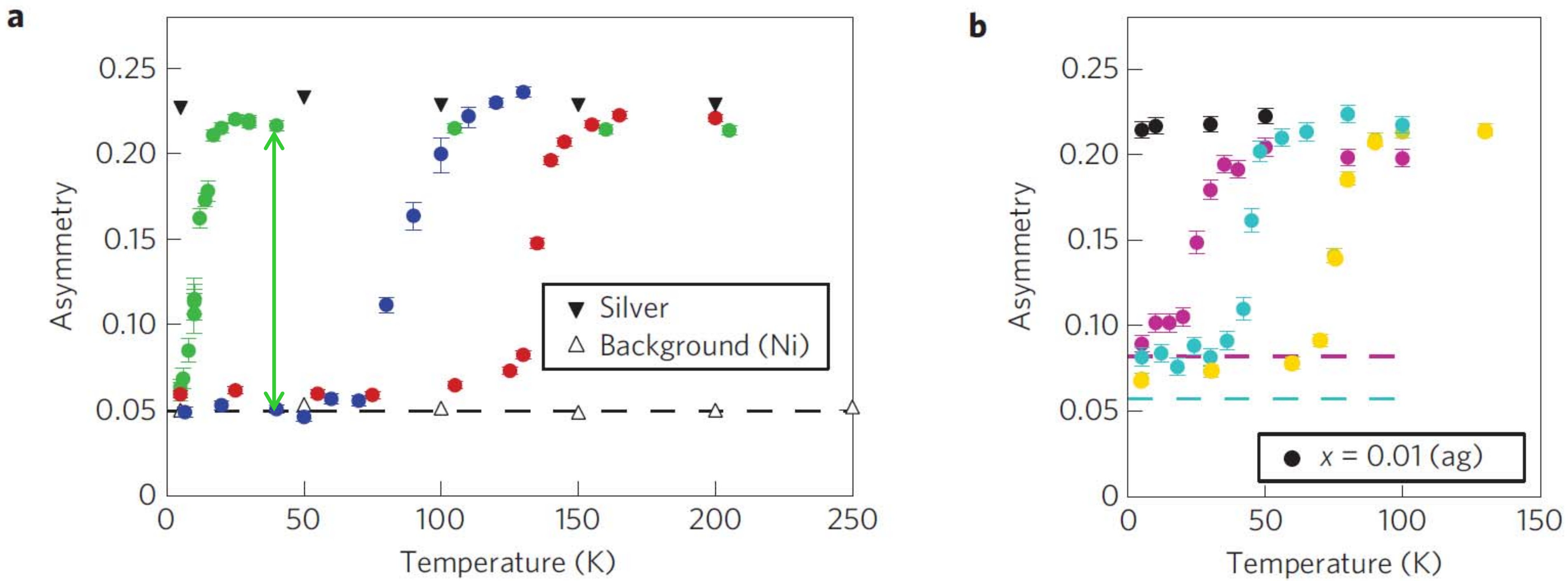

FM of properly grown samples is homogeneous

S. Dunsiger et al., Nature Materials **9**, 299 (2010)

Examples III

- Buried or spacer layers

- Probing the electron polarization $\langle s_e(x) \rangle$ in Fe/Ag/Fe and in an organic spin valve

- Fourier transform of P(t) → field distribution p(B) → spatial variation of electron polarization $\langle s_e(x) \rangle$

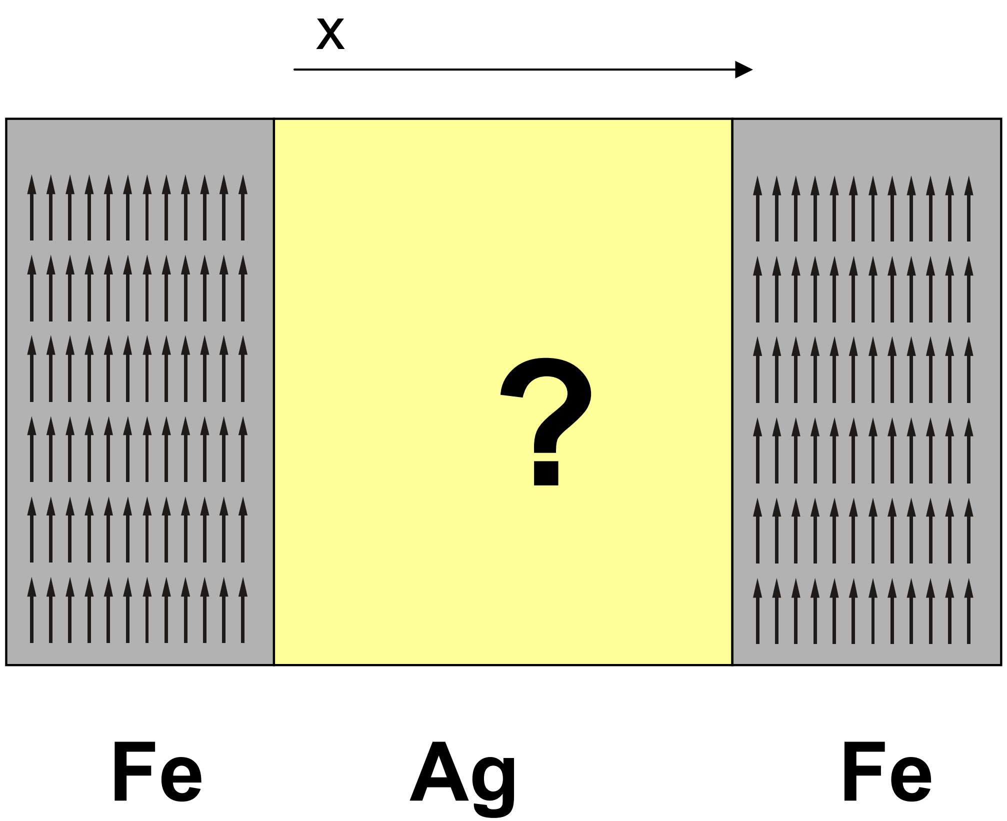

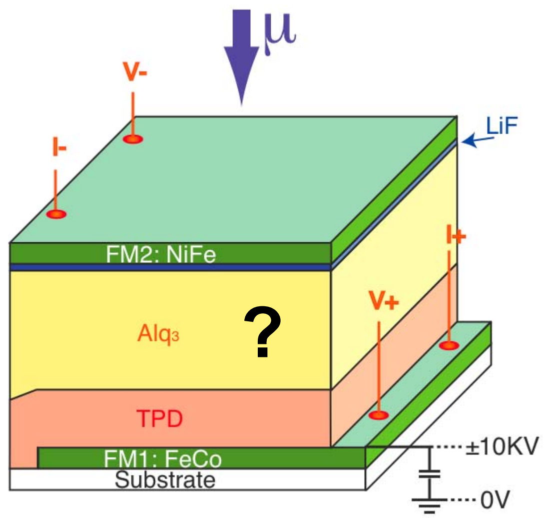

Contributions to local field B_μ

Muons measure local fields generated by: moments, spins, (super)currents,..

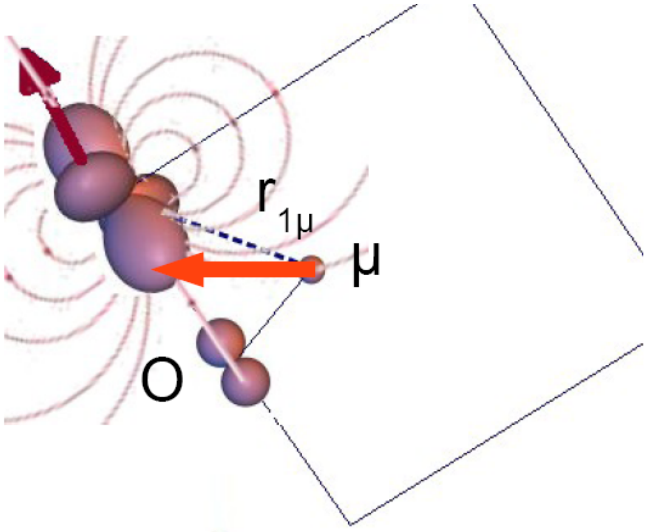

Dipolar field from a localized moment:

$$\vec{B}_{dip}(\vec{r}_i) = \frac{\mu_0}{4\pi} \frac{3(\vec{\mu}_i \cdot \vec{r}_i) \cdot \vec{r}_i - \vec{\mu}_i r_i^2}{r_i^5}$$

$$B_{dip} \approx \frac{\mu_0}{4\pi} \frac{\mu_i}{r_{1\mu}{}^3} \approx \frac{\mu_i[\mu_B]}{d^3[A^3]}\ \mathrm{T} \quad \text{(typical 0.1 T,}$$

dominant term in magnetic materials)

Contact field (determined by electron

spin polarization at muon position r=0):

$$B_c = \mu_0 \frac{2}{3} g_e \mu_B < s_z > |\phi(0)|^2 \quad \propto \quad A$$

$(\leftrightarrow$ contact interaction $H = A\, \vec{s}_\mu \cdot \vec{s}_e)$

(Magnetized sphere M gives field $B = \mu_0 \frac{2}{3} M$)

Sources of electron polarization

-External field in simple metals→ Pauli paramagnetism of conduction electrons

-Magnetic moments (layers) interacting via polarization of conduction electrons→ RKKY interaction

-Spin injection: Polarized electrons injected/tunneling from a FM into a non-magnetic layer

-….

RKKY interaction

Interaction between two moments via oscillating polarization of conduction electrons

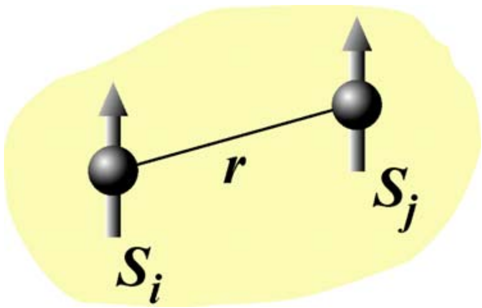

$$\mathcal{H}_{\mathrm{RKKY}} = -J(r)\; \boldsymbol{S_i} \cdot \boldsymbol{S_j}$$

$$J(r) \propto \frac{1}{r^3} \cos(2k_F r + \phi)$$

(leading term for spherical FS. Details depend on Fermi surface)

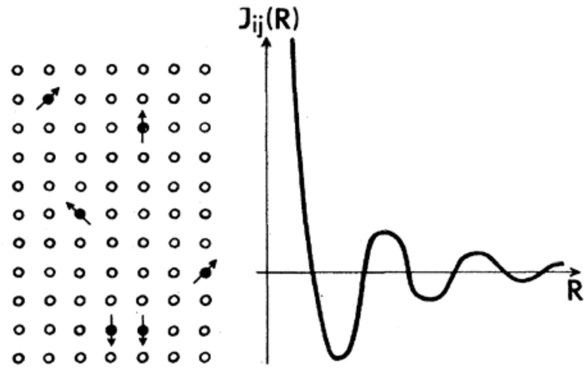

Two magnetic layers: Integrate RKKY over interfaces →

Oscillating polarization of the conduction electrons →

Interlayer exchange coupling oscillates with thickness d

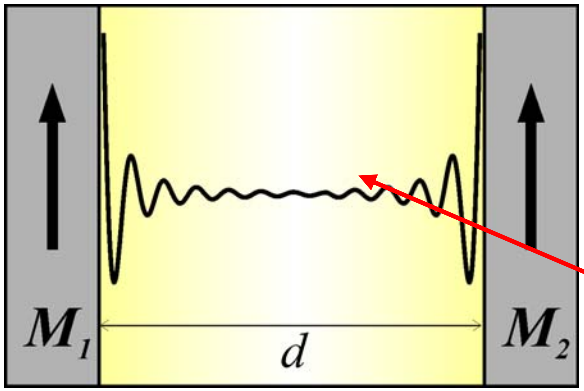

$$J(d) \propto \frac{1}{d^2} \cos(qd + \phi)$$

$$E = -J(d)\; \boldsymbol{M_1} \cdot \boldsymbol{M_2}$$

Muons probe the oscillating electron polarization of the nonmagnetic spacer (Spin Density Wave) mediating the coupling between the FM layers.

Oscillating polarization of conduction electrons

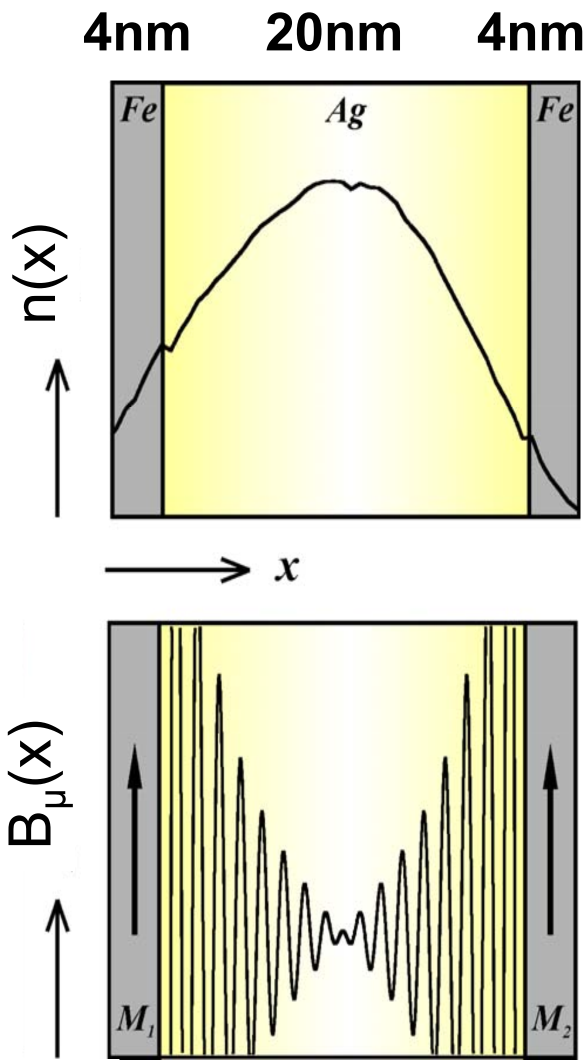

Fe/Ag/Fe

Implantation profile of 3 keV muons

Oscillating polarization of conduction electrons $<s_z(x)>$ produces an oscillating contact field $B_{spin}(x) \propto <s_z(x)>$

The depth resolution of LE-μSR cannot resolve the oscillations (WL ~ 1 nm or less), but the oscillating behavior is reflected in the field distribution $p(B_\mu)$ sensed by the muons.

H. Luetkens, J. Korecki, E. Morenzoni, T. Prokscha, M. Birke, H. Glückler, R. Khasanov, H.-H. Klauss, T. Slezak, A. Suter, E. M. Forgan, Ch. Niedermayer, and F. J. Litterst Phys Rev. Lett. **91**, 017204 (2003).

Relation muon spin polarization - field distribution

Formula for "static" fields (A. Amato lecture):

$$P_z(t) = \int p(\mathbf{B}_\mu)\left[\cos^2\theta + \sin^2\theta\cos(\gamma_\mu B_\mu t + \phi)\right] d\mathbf{B}_\mu$$

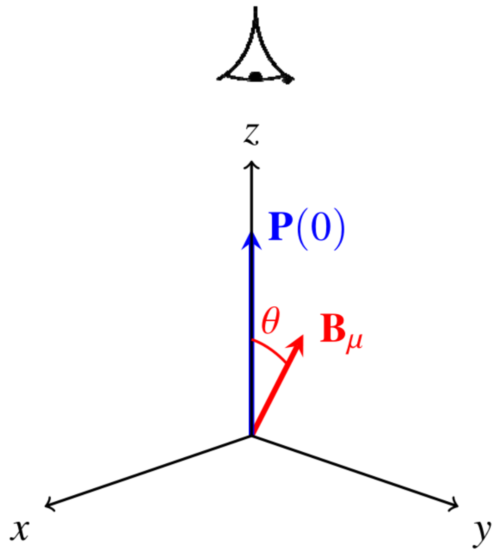

In our case: TF θ=90, $B_\mu = B_{ext} + B_{spin}(x)$ || x

$$A(t) \propto P_z(t) = \int p(B_\mu)\cos(\gamma_\mu B_\mu t + \phi) dB_\mu$$

$P_z(t)$ is the cosine Fourier transform of the magnetic field distribution

$p(B_\mu)$ can be obtained by fast Fourier transform, maximum entropy method, or modeled and fitted in time domain

LE-μSR on Fe/Ag/Fe: Time domain

$$A(t) \propto P_z(t) = \int p(B_\mu)\cos(\gamma_\mu B_\mu t + \phi)\,dB_\mu$$

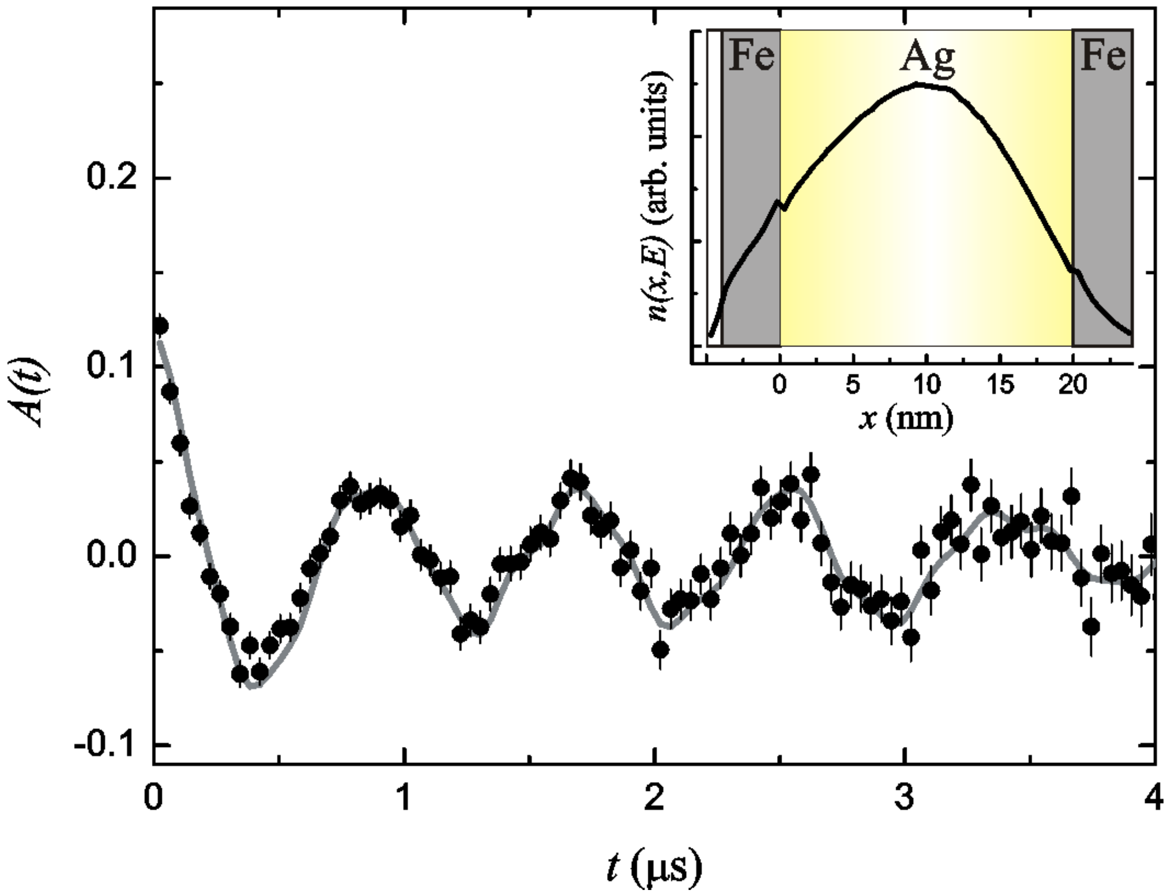

Field distribution

$$B_\mu = B_{ext} + B_{spin}(x)$$

LE-μSR on Fe/Ag/Fe: Field domain

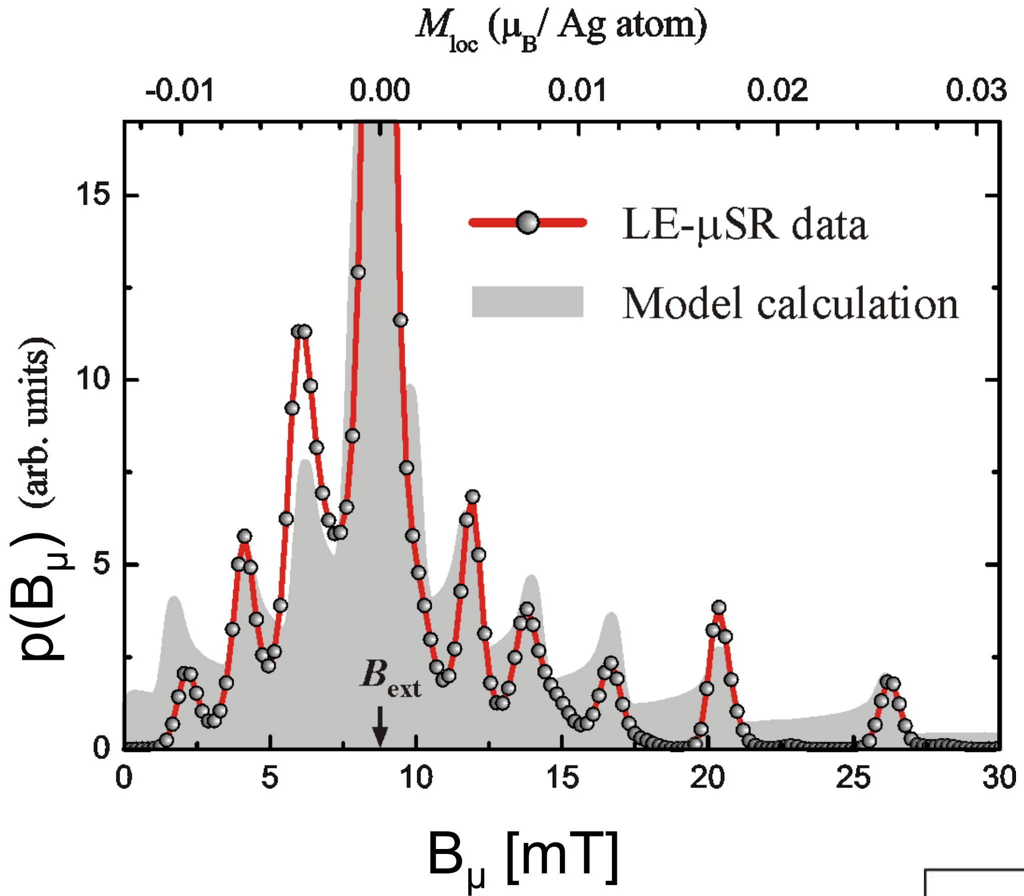

Alternating positive and negative $B_{spin}(x)$ contributions (contact field)

Turning points of oscillations produce side bands to the B_{ext}

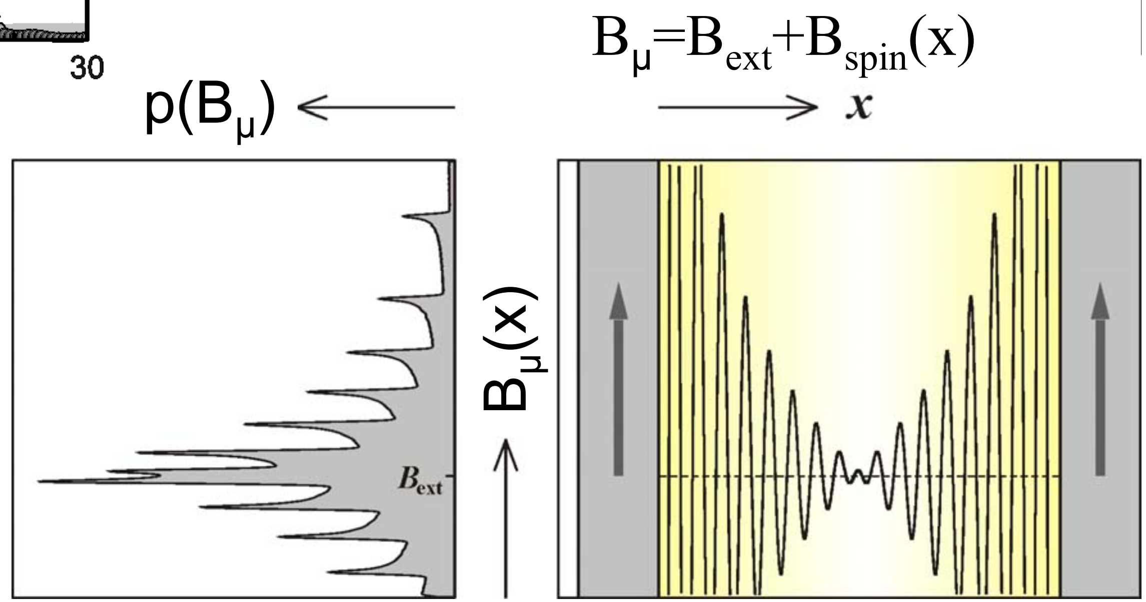

H. Luetkens et al, Phys. Rev. Lett. ***91*** *(2003) 017204.*

LE-μSR on Fe/Ag/Fe: Field domain

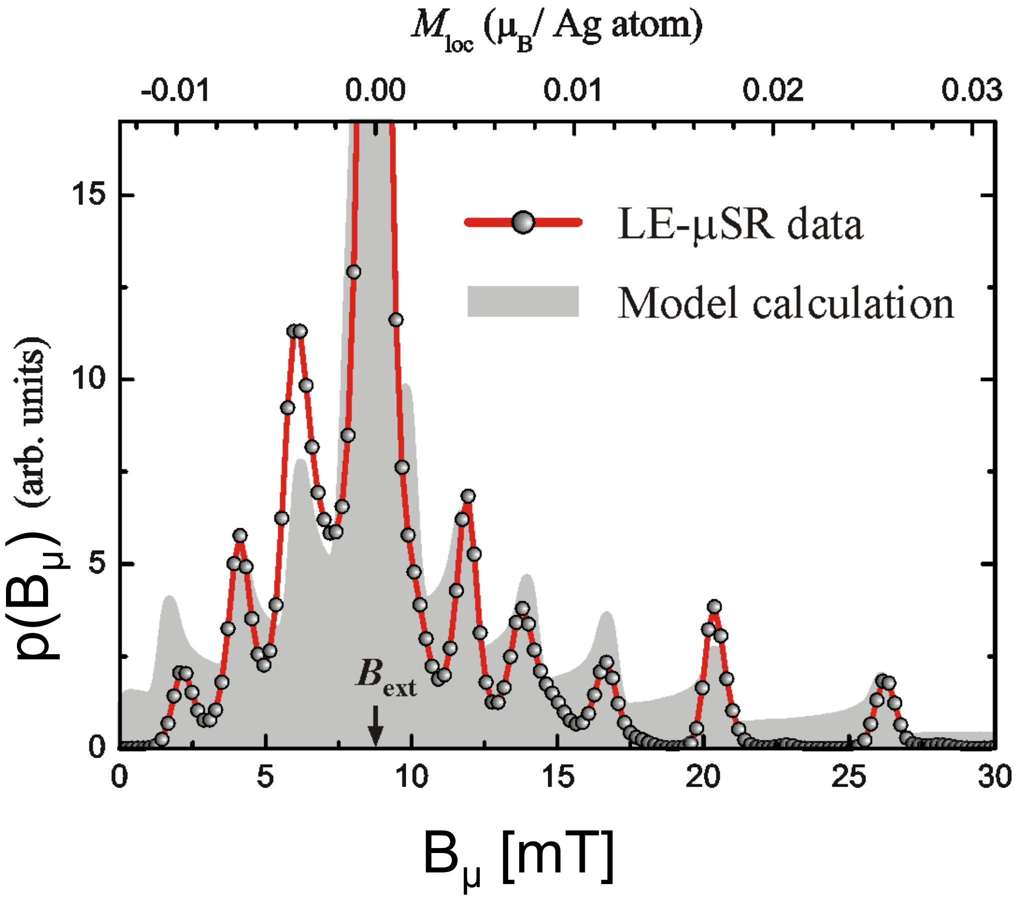

Results:

- From p(B_μ) → Oscillating electron spin polarization $<s_z(x)>$ within Ag

- $<s_z(x)>$ and IEC oscillate with the same period, determined by the Ag FS

- Attenuation of electron spin polarization: significantly smaller than the one of IEC strength (beyond RKKY: confined electron states in a quantum well model)

$$B_{spin}(x) \propto < s_z(x) > = \sum_{i=1}^{2} C_i \sin(q_i x + \varphi_i) \frac{1}{x^{\alpha_i}}$$

$$\alpha = 0.8(1)$$

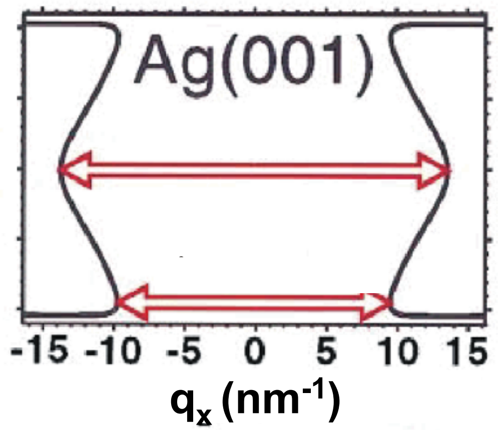

H. Luetkens et al, Phys. Rev. Lett. ***91*** *(2003) 017204.*

Probing spin injection in an organic spin valve

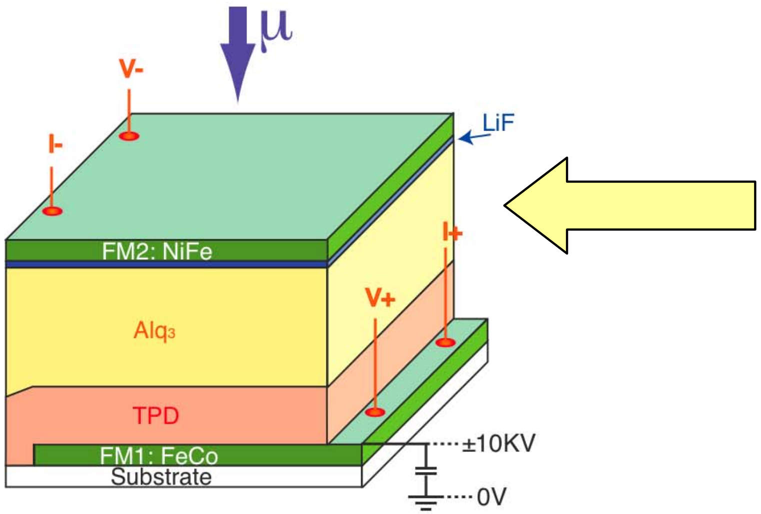

Spacer:
organic semiconductor
Alq3: $C_{27}H_{18}N_3O_3Al$

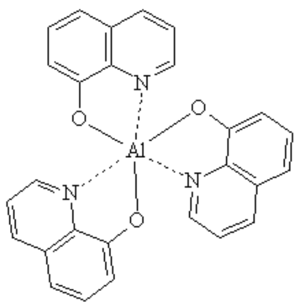

Magnetoresistance and Hysteresis

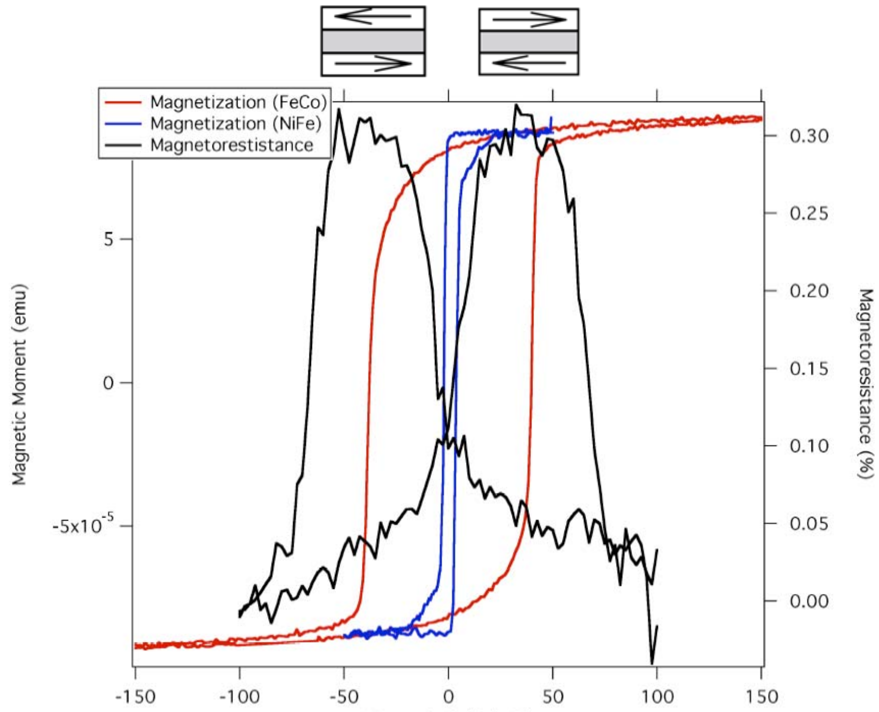

B_{appl}

$$MR = \frac{\Delta R}{R} = \frac{R_{AP} - R_P}{R_{AP}}$$

A. Drew et al. Nature Materials **8**, 109-114 (2009)

Giant magnetoresistance in organic spin valves

MR vs thickness

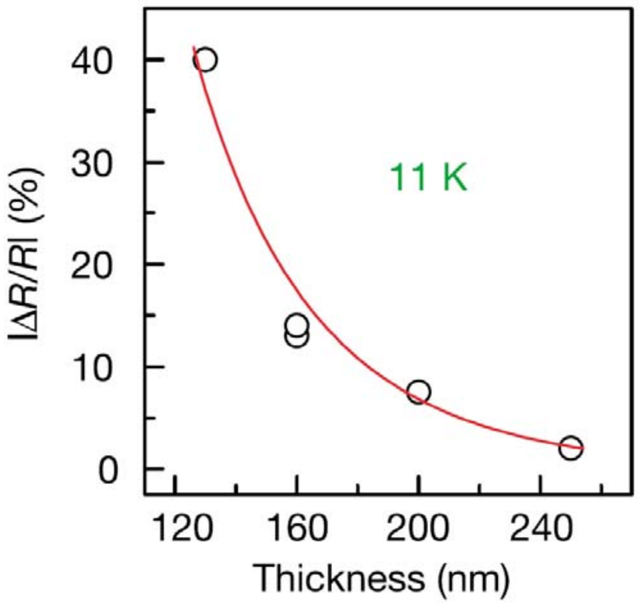

Magnetoresistance vs T

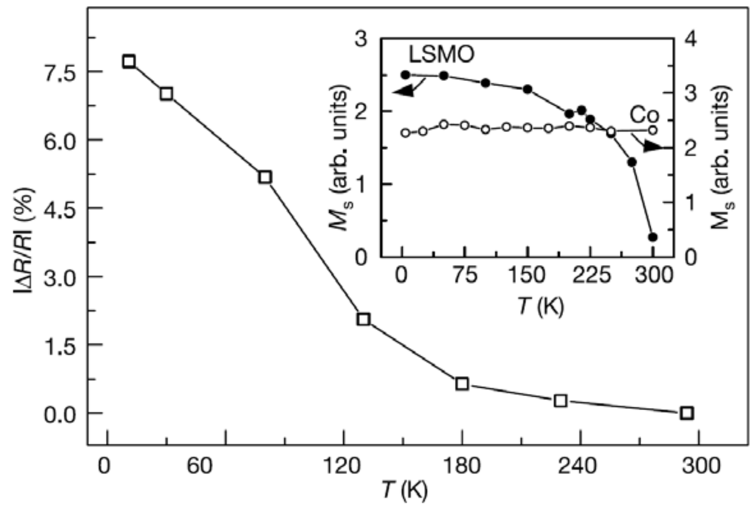

Z.H. Xiong et al.,Nature **427**, 821 (2004)

$$MR = \frac{\Delta R}{R} = \frac{R_{AP} - R_P}{R_{AP}}$$

Goal of experiment:

Better understand spin injection (e.g. diffusion length) and its relation to MR in organic SV

GMR:

1988: Discovered in metallic multilayers

2007: Nobel Prize A. Fert, P. Grünberg

1997: First application: read sensors of hard disks

Principle of the LE-μSR experiment

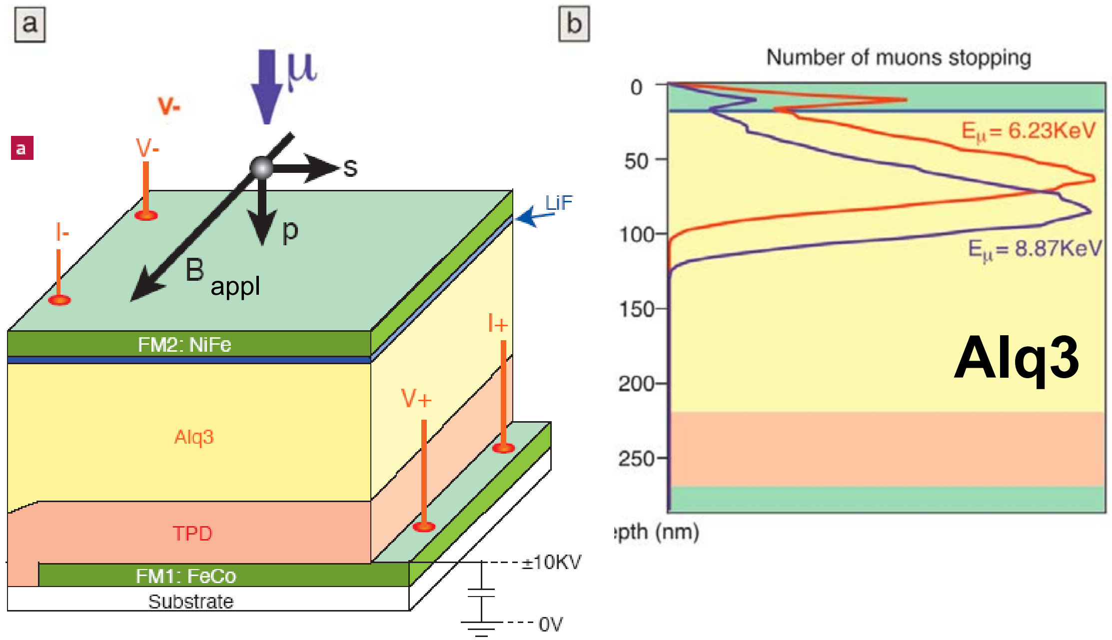

Spin injection detected by shape analysis of local field distribution $p(B_\mu)$

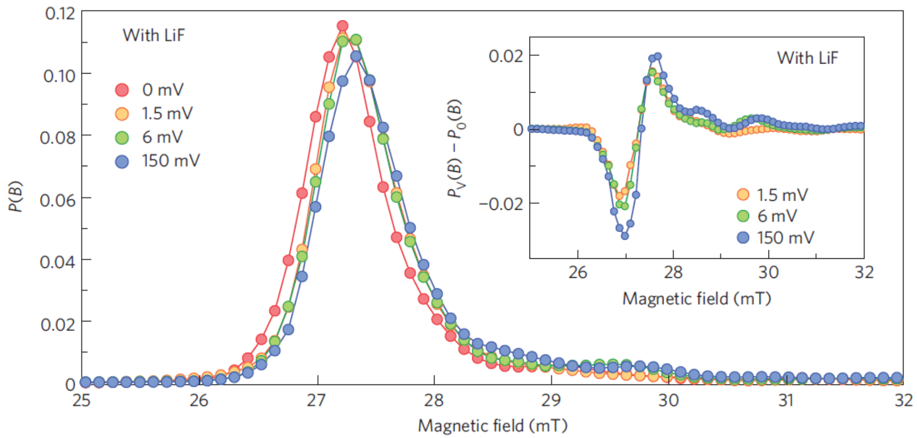

-Injected spins have long spin coherence time ~10^{-5} s >> τ_μ

-In the organic material they produce static field $B_{spin} \propto \langle s_z(x)\rangle$ that adds to B_{appl} used to select spin valve state

-B_μ is detected by muons stopped at various depths → $p(B_\mu)$

-The B_{spin} component can be separated by switching on/off the injection with I (V) and changing its sign with respect to B_{appl}

The LE-μSR experiment

$p(B_\mu)$ field distribution

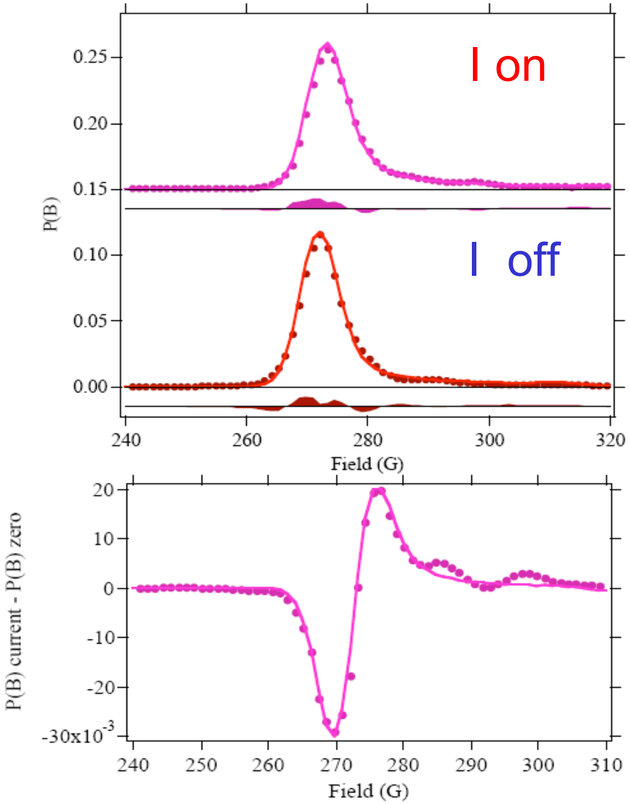

field distributions: I_{on} - I_{off}

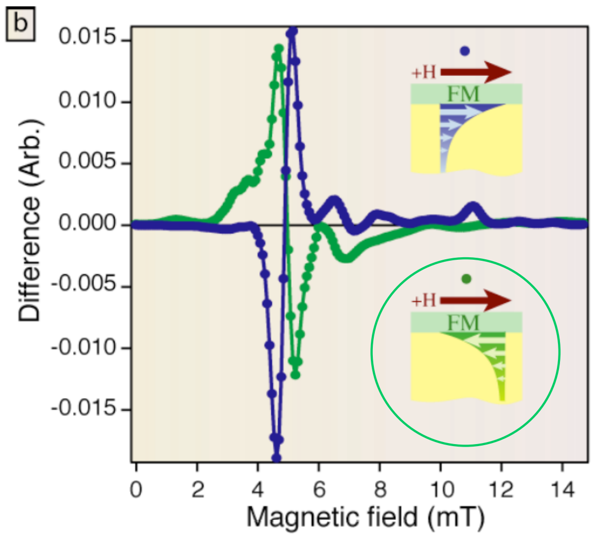

Magnetoresistance

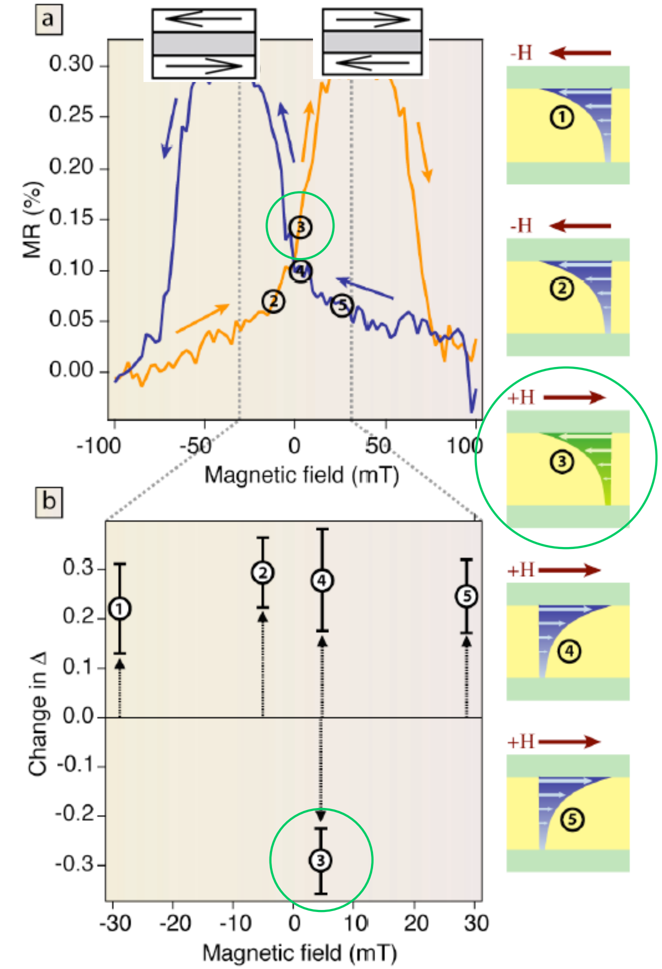

Skewness

Spin diffusion length in organic spin valve

Spin injection detected by shape analysis of local field distribution $p(B_\mu)$

First direct measurement of spin diffusion length in a working spin valve.

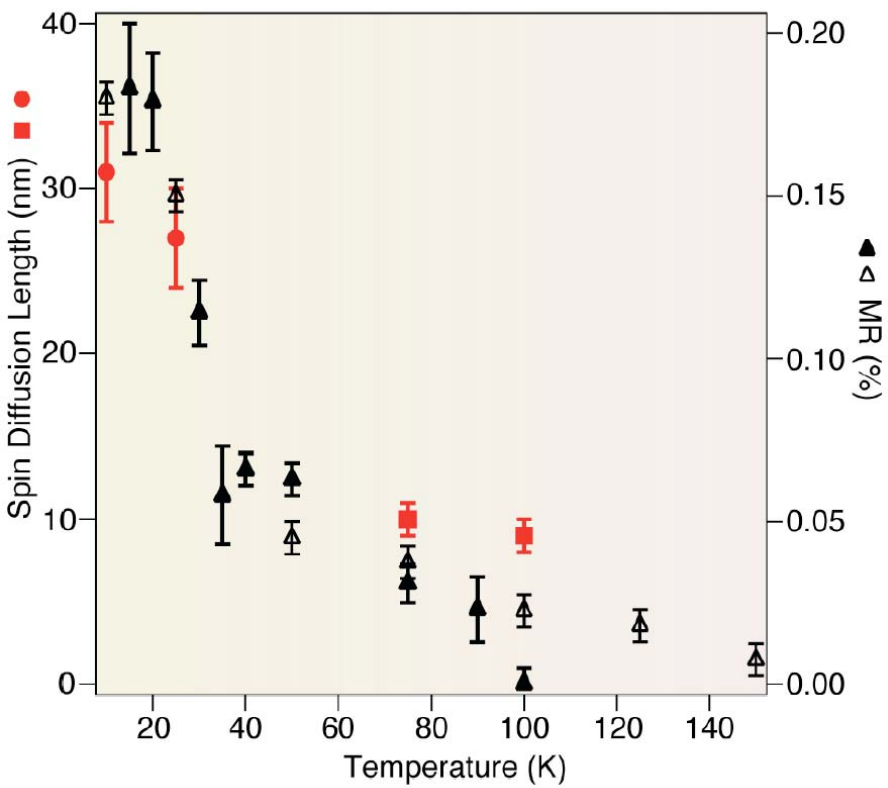

- Temperature dependence of spin diffusion length correlates with magnetoresistance
- Polarization of injected carriers can be reversed by 1-nm thin polar LiF layer at the interface

A. Drew et al. Nature Materials **8**, 109 (2009)

L. Schultz et al. Nature Materials **10**, 39 (2011)

Example IV: Probing dynamics

Change in polarization P(t) is caused by:

1) Distribution of local fields $p(B_{\mu})$ → dephasing (“static” fields)

2) Exchange of energy between muon spin and the system under study (dynamics)

Dynamics: spin fluctuations, current fluctuations, molecular motion, muon diffusion,….

Up to now examples of category 1)

One example of 2)

Muon in a fluctuating environment

$B_\mu = B_{ext} + B_{fl}(t)$

Fluctuating term $\langle B_{fl}(t)\rangle = 0$

but $\langle \Delta B_i(t)^2 \rangle \neq 0$

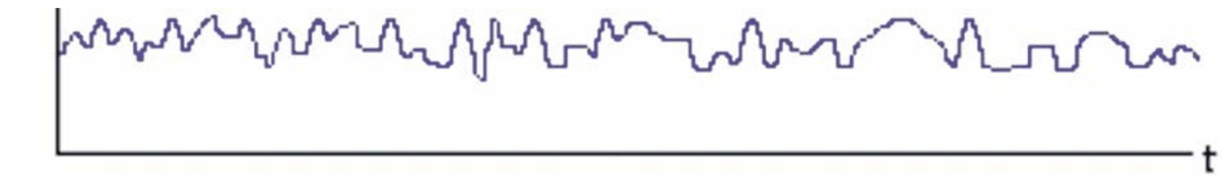

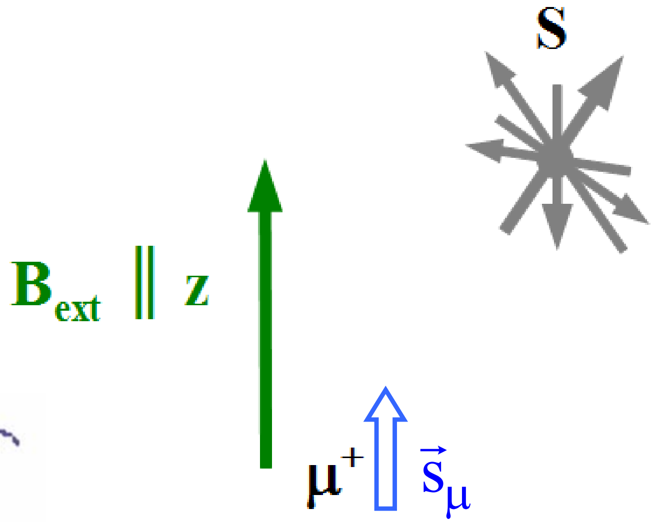

Zeeman splitting in B_{ext}:

$$\Delta E = 2\mu_\mu B_{ext} = 2 s_\mu \gamma_\mu B_{ext} = \hbar\omega_L \qquad \text{(neV-}\mu\text{eV !)}$$

$$H = -\vec{\mu}_\mu \vec{B} = -\gamma_\mu (\vec{B}_{ext} + \vec{B}_{fl}(t))\hbar\vec{s}_\mu$$

Muon in a fluctuating environment

$B_\mu = B_{ext} + B_{fl}(t)$

At t=0: P(0)=1 i.e. all muons in m=+1/2 state

$B_{fl}(t)$ induces transitions between the Zeeman states

→ muon spin relaxation $P(t) = P(0)\, e^{-\lambda t}$

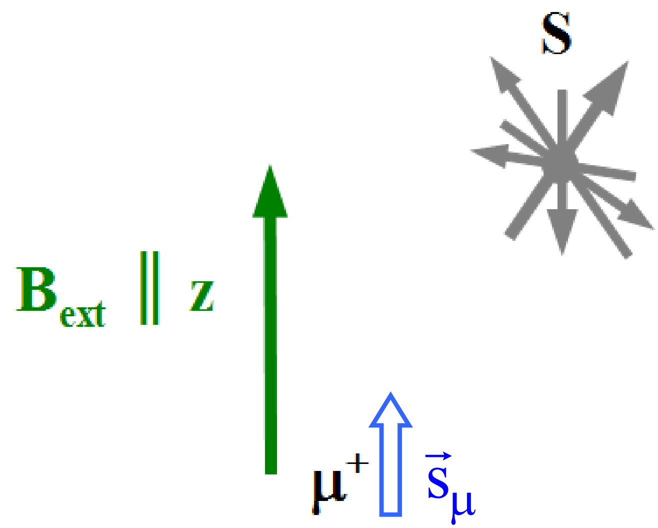

Zeeman splitting in B_{ext}:

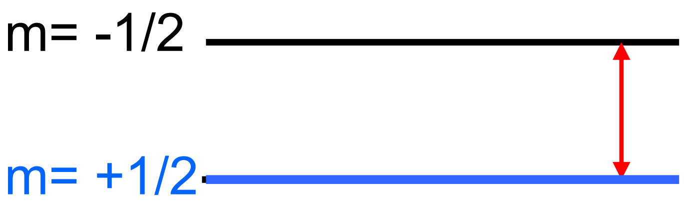

$$\Delta E = 2\mu_\mu B_{ext} = 2 s_\mu \gamma_\mu B_{ext} = \hbar\omega_L \qquad \text{(neV-}\mu\text{eV !)}$$

$$H = -\vec{\mu}_\mu \vec{B} = -\gamma_\mu (\vec{B}_{ext} + \vec{B}_{fl}(t)) \hbar \vec{s}_\mu$$

Muon in a fluctuating environment

The relaxation rate is a function of the field fluctuations.
Field fluctuations characterized by autocorrelation function.
(Redfield theory, see e.g. C. Slichter, Principles of nuclear magnetic resonance)

$$\lambda = \frac{1}{T_1} = \frac{\gamma_\mu^2}{2} \int_{-\infty}^{\infty} (< B_x(t) B_x(t+t') > e^{i\omega_L t'} + < B_y(t) B_y(t+t') > e^{i\omega_L t'}) dt'$$

$$\vec{B}_{ext} || \vec{P}(0) || \hat{z}$$

The longitudinal relaxation rate is proportional to the Fourier transform of the correlation function of the local field, evaluated at the Larmor frequency.
The muon spin relaxation is an intrinsically resonant phenomenon.

(In many cases the field correlation function $<B_i\ B_i>$ reflects the electronic spin autocorrelation function $<S_i\ S_i>$)

Correlation time

In case of exponential autocorrelation function with one correlation time:

$$< B_q(t) B_q(t+t') > = < B_q^2(0) > e^{-\frac{t'}{\tau_c}} \cong$$

$$< S_q(t) S_q(t+t') > = < S_q(0)^2 > e^{-\frac{t'}{\tau_c}}$$

$$\lambda = \gamma_\mu^2 (< B_x^2 > + < B_y^2 >) \frac{\tau_c}{1+\omega_L^2 \tau_c^2}$$

For fluctuating Gauss distributed fields (with width $<\Delta B_\mu^2>$)
produced by fluctuating spins with a fluctuation time τ_c
the muon spin relaxation rate is given by:

$$\lambda = 2\gamma_\mu{}^2 < \Delta B_\mu{}^2 > \frac{\tau_c}{1+\omega_L{}^2 \tau_c{}^2} \qquad P(t)=P(0)e^{-\lambda t}$$

Slowing down of fluctuations

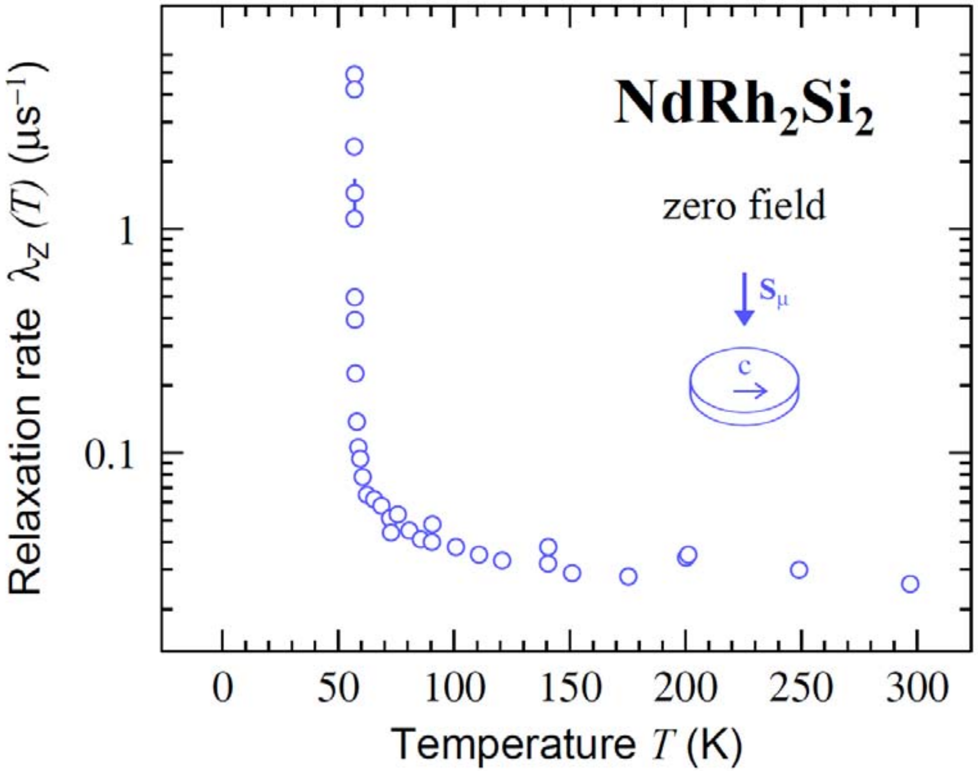

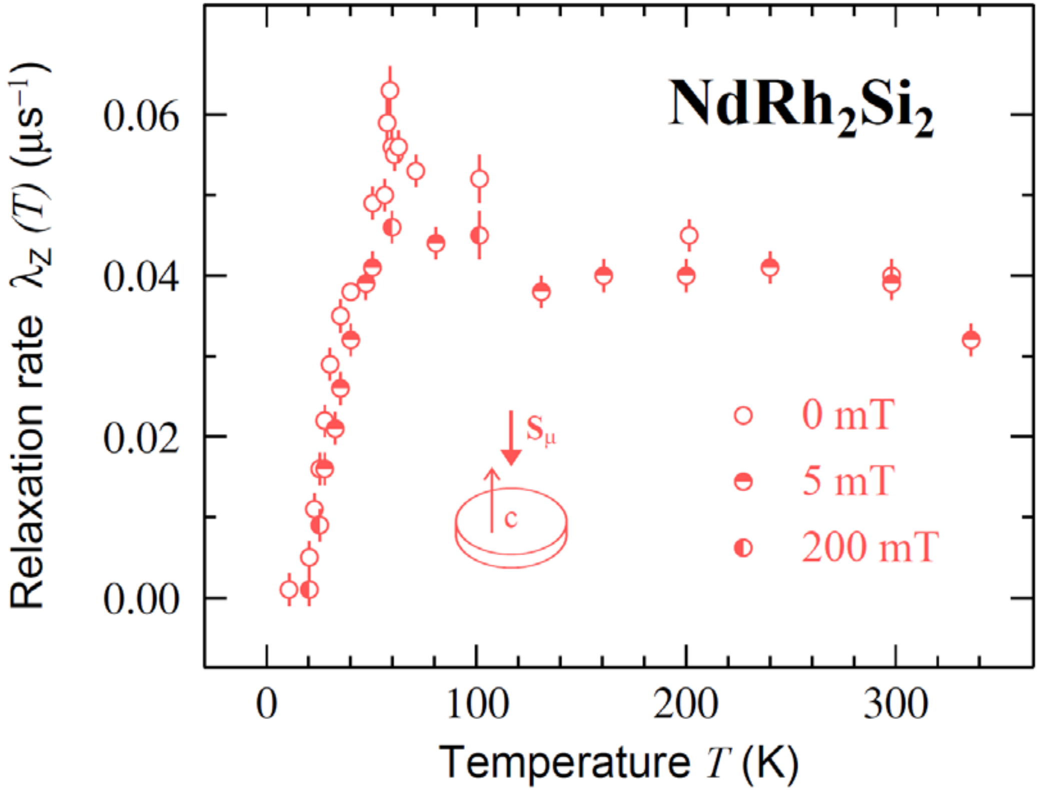

Large increase of λ_Z ($s_\mu \perp c$) when T → T_N^+ (57 K): critical slowing down of magnetic fluctuations ($\lambda_Z \propto \tau_c$)

Anisotropy of $\lambda_Z(T)$ reflects anisotropy of fluctuations

Freezing in Spin Glasses

Spin Glass: a system with disorder and frustration

Example: canonical Spin Glasses *AuFe*, *CuMn*, *AgFe* (1-5 at%)

Randomness (site disorder) and oscillating RKKY interaction → competition, frustration

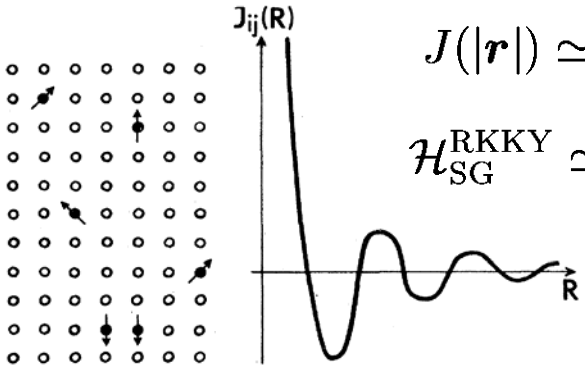

$$J(|\boldsymbol{r}|) \simeq J_0 \frac{\cos(2k_F r + \phi)}{(2k_F r)^3}$$

$$\mathcal{H}_{SG}^{RKKY} \simeq -\sum_{R_{ij}=|\boldsymbol{r}_i-\boldsymbol{r}_j|} J(R_{ij})\ \boldsymbol{S}_i \cdot \boldsymbol{S}_j$$

Cooperative freezing at T_f
with static moment formation, but
no long range order

$< S_i >_t \neq 0$ $\quad$ S_i impurity spin

$$\frac{1}{N}\sum < S_i >_t e^{i\vec{k}\vec{r}} = 0 \qquad N \rightarrow \infty$$

$< >_t$ $\quad$ time average $t >> t_{meas}$

CuMn(1%)

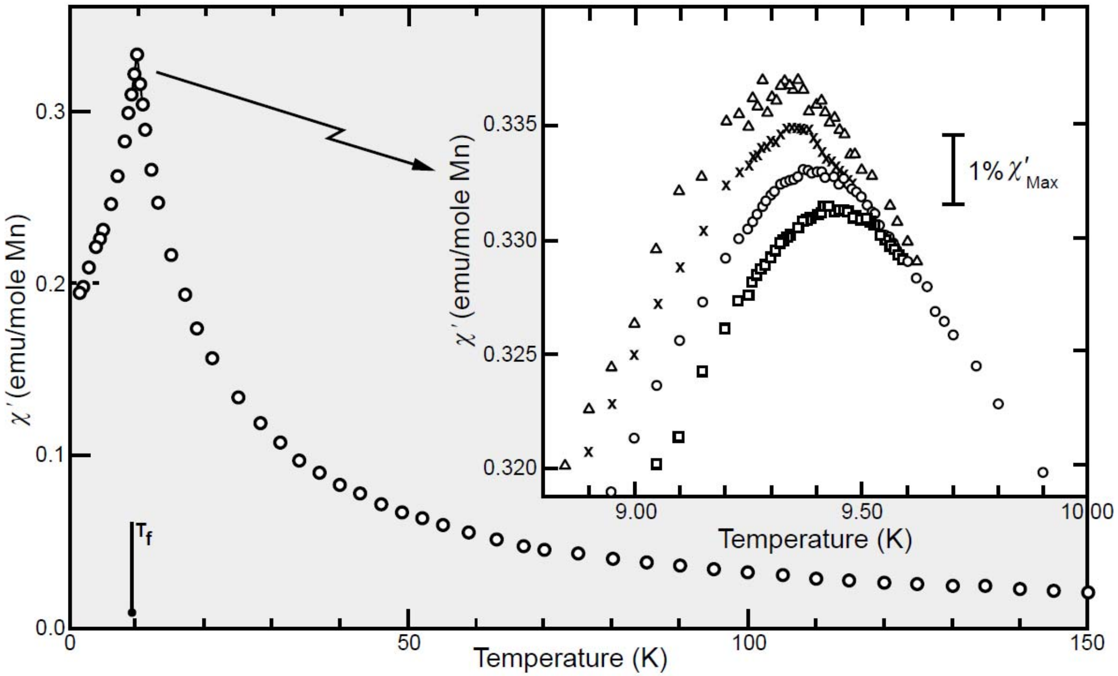

C. Mulder et al., PRB23, 1384 (1981)

Dimensional effects in spin glasses

$$P(t) = P(0)\, e^{-(\lambda t)^{\beta}}$$

Thickness dependence

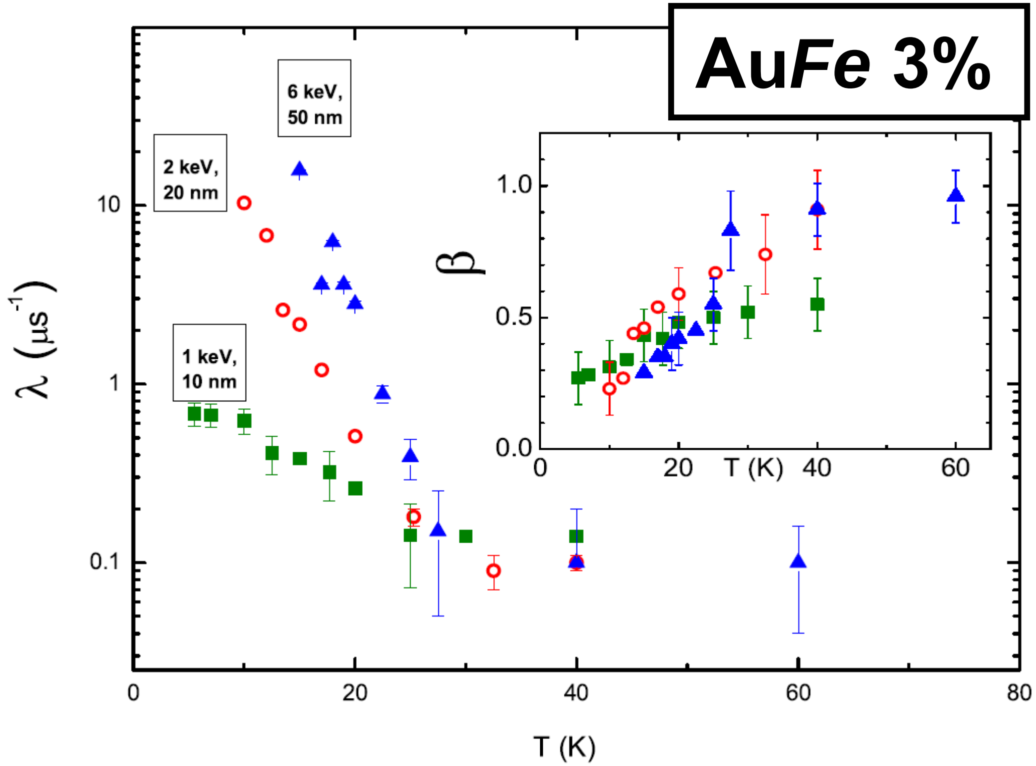

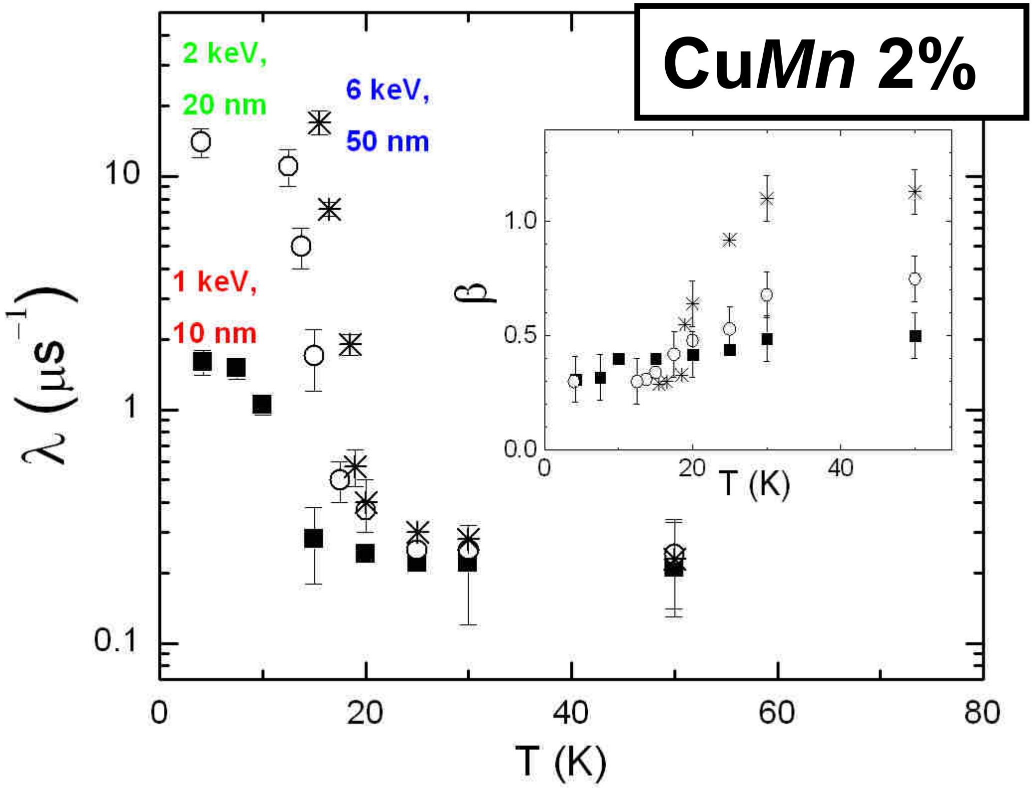

Reduction of λ with thickness and….

AuFe(3%) 220 nm: depth dependence

$$P(t) = P(0)\, e^{-(\lambda t)^{\beta}}$$

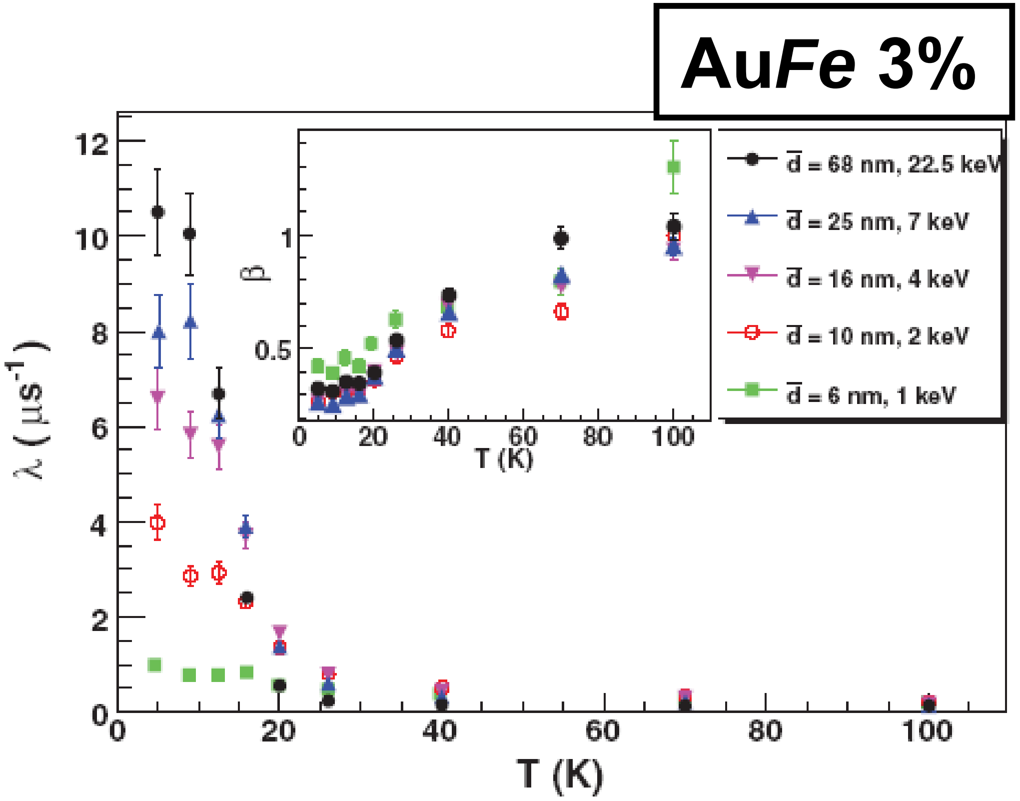

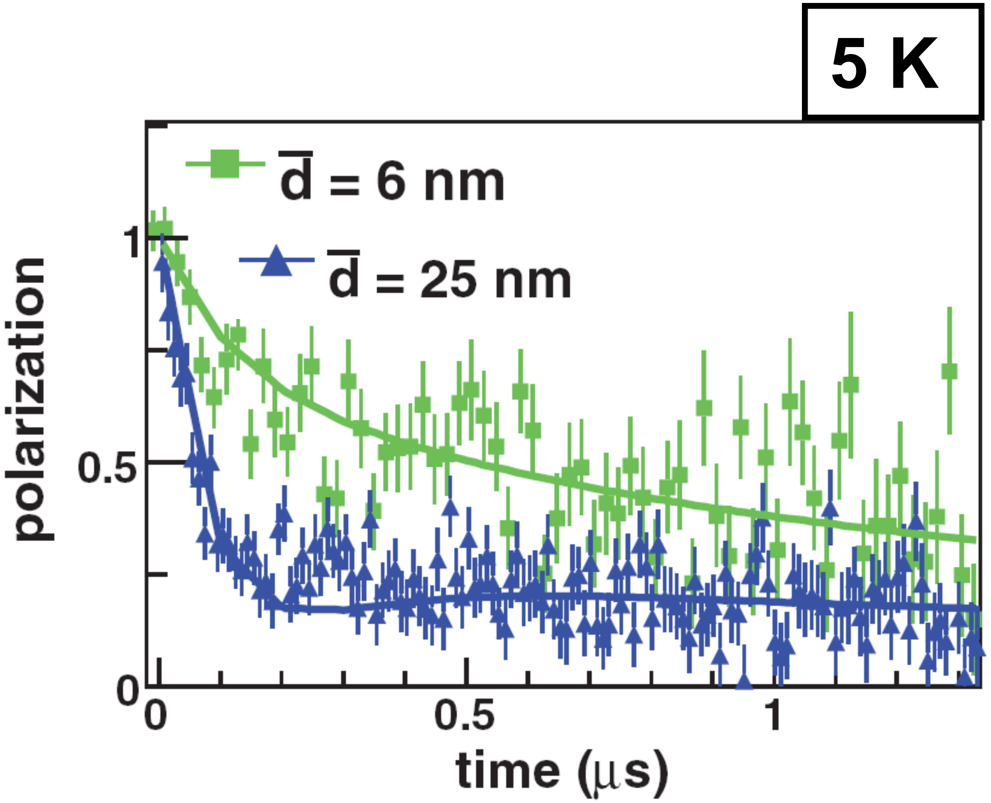

…..and depth

Cooperative freezing at similar T_f as in bulk but increasing dynamics on approaching the surface (length scale ~10 nm) and reduction of order parameter (static moment)

E. Morenzoni, H. Luetkens, A. Suter, Th. Prokscha, S. Vongtragool, F. Galli, M. Hesselberth, N. Garifianov, R. Khasanov
Physical Review Letters **100**, 147205 (2008)

Polarized muons are sensitive local probes of magnetic, superconducting and.. properties

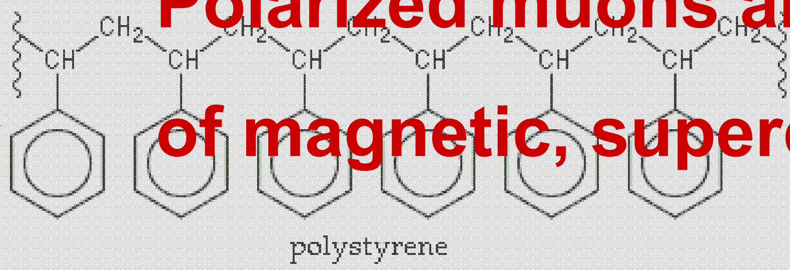

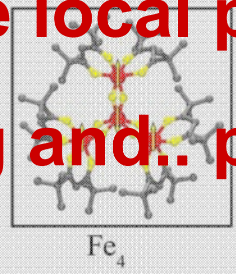

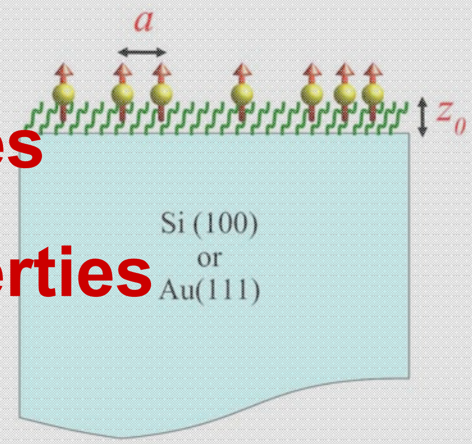

Static and dynamic

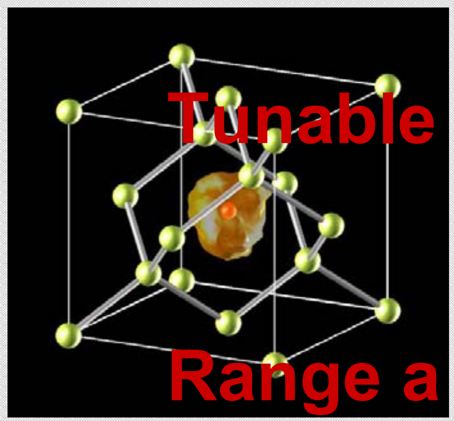

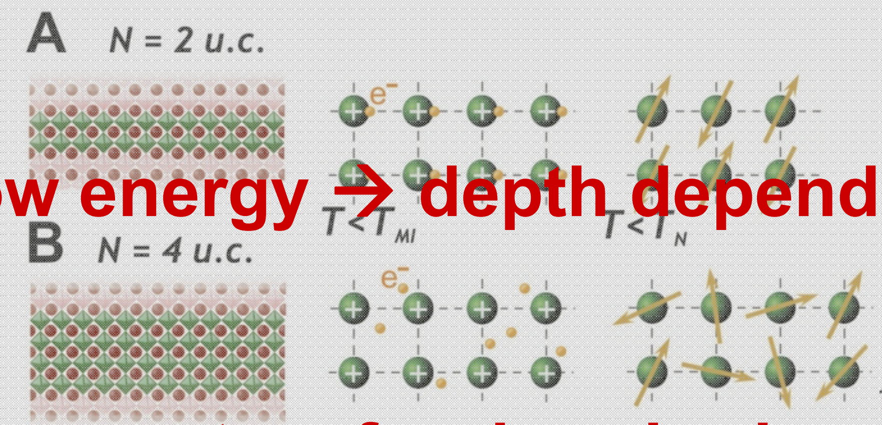

Tunable low energy → depth dependent investigations

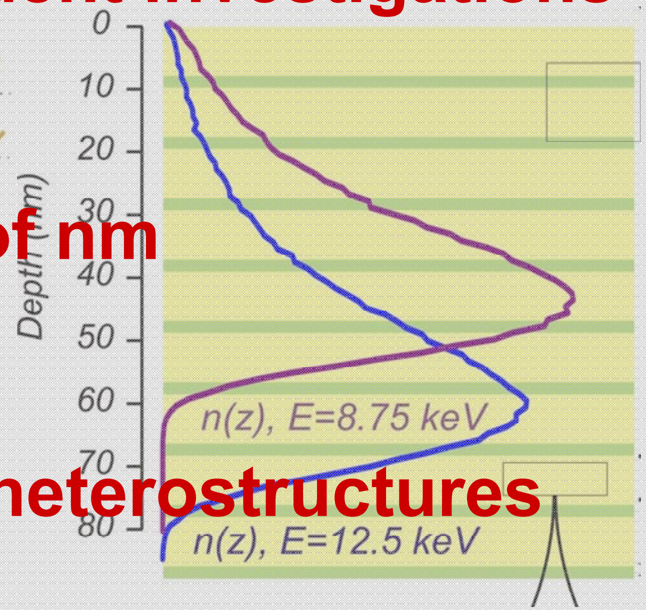

Range a few nm to a few hundreds of nm

→ Thin films, near surface regions, heterostructures

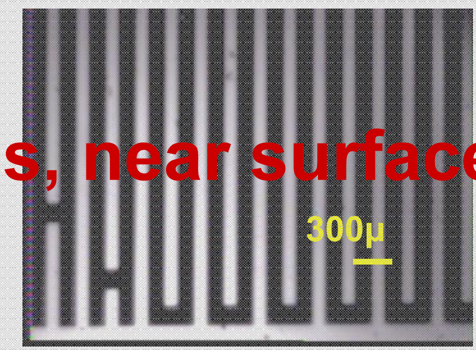

Thank you!

Literature

BOOKS

•A. Yaouanc, P. Dalmas de Réotier, MUON SPIN ROTATION, RELAXATION and RESONANCE (Oxford University Press, 2010)

•A. Schenck, MUON SPIN ROTATION SPECTROSCOPY, (Adam Hilger, Bristol 1985)

•E. Karlsson, SOLID STATE PHENOMENA, As Seen by Muons, Protons, and Excited Nuclei, (Clarendon, Oxford 1995)

•S.L. Lee, S.H. Kilcoyne, R. Cywinski eds, MUON SCIENCE: MUONS IN PHYSICS; CHEMISTRY AND MATERIALS, (IOP Publishing, Bristol and Philadelphia, 1999)

•INTRODUCTORY ARTICLES

•S.J. Blundell, SPIN-POLARIZED MUONS IN CONDENSED MATTER PHYSICS, Contemporary Physics 40, 175 (1999)

•P. Bakule, E. Morenzoni, GENERATION AND APPLICATIONN OF SLOW POLARIZED MUONS, Contemporary Physics 45, 203-225 (2004).

REVIEW ARTICLES, APPLICATIONS

•P. Dalmas de Réotier and A. Yaouanc, MUON SPIN ROTATION AND RELAXATION IN MAGNETIC MATERIALS, J. Phys. Condens. Matter 9 (1997) pp. 9113-9166

•A. Schenck and F.N. Gygax, MAGNETIC MATERIALS STUDIED BY MUON SPIN ROTATION SPECTROSCOPY, In: Handbook of Magnetic Materials, edited by K.H.J. Buschow, Vol. 9 (Elsevier, Amsterdam 1995) pp. 57-302

•B.D. Patterson, MUONIUM STATES IN SEMICONDUCTORS, Rev. Mod. Phys. 60 (1988) pp. 69-159

•A. Amato, HEAVY-FERMION SYSTEMS STUDIED BY μSR TECHNIQUES, Rev. Mod. Phys., 69, 1119 (1997)

•V. Storchak, N. Prokovev, QUANTUM DIFFUSION OF MUONS AND MUONIUM ATOMS IN SOLIDS, Rev. Mod. Physics, 70, 929 (1998)

•J. Sonier, J. Brewer, R. Kiefl, μSR STUDIES OF VORTEX STATE IN TYPE-II SUPERCONDUCTORS, Rev. Mod. Physics, 72, 769 (2000)

•E. Roduner, THE POSITIVE MUON AS A PROBE IN FREE RADICAL CHEMISTRY, Lecture Notes in Chemistry No. 49 (Springer Verlag, Berlin 1988)